

Emergence of density dynamics by surface interpolation in elementary cellular automata



Juan Carlos Seck-Tuoh-Mora^{a,*}, Joselito Medina-Marin^a, Genaro J. Martínez^{b,c}, Norberto Hernández-Romero^a

^a Area Académica de Ingeniería, Universidad Autónoma del Estado de Hidalgo, Carr. Pachuca Tulancingo Km. 4.5, Pachuca Hidalgo 42184, Mexico

^b Departamento de Ciencias e Ingeniería de la Computación, Escuela Superior de Computo, Instituto Politécnico Nacional, Av. Miguel Othon de Mendizábal s/n., Mexico D.F. 07738, Mexico

^c Unconventional Computing Center, Bristol Institute of Technology, University of the West of England, Bristol BS16 1QY, United Kingdom

ARTICLE INFO

Article history:

Received 27 February 2013

Received in revised form 29 May 2013

Accepted 14 August 2013

Available online 24 August 2013

Keywords:

Cellular automata classification

Mean field theory

Basins of attraction

Density behaviour

Surface interpolation

ABSTRACT

A classic problem in elementary cellular automata (ECAs) is the specification of numerical tools to represent and study their dynamical behaviour. Mean field theory and basins of attraction have been commonly used; however, although the first case gives the long term estimation of density, frequently it does not show an adequate approximation for the step-by-step temporal behaviour; mainly for non-trivial behaviour. In the second case, basins of attraction display a complete representation of the evolution of an ECA, but they are limited up to configurations of 32 cells; and for the same ECA, one can obtain tens of basins to analyse. This paper is devoted to represent the dynamics of density in ECAs for hundreds of cells using only two surfaces calculated by the nearest-neighbour interpolation. A diversity of surfaces emerges in this analysis. Consequently, we propose a surface and histogram based classification for periodic, chaotic and complex ECA.

© 2013 Elsevier B.V. All rights reserved.

1. Introduction

Elementary cellular automata (ECAs) have been widely studied because they are able to produce interesting dynamical behaviour based on very simple local interactions [1,2].

A classic problem in ECAs has been the specification of numerical tools and methods to analyse, predict and classify their dynamical behaviour.

The use of mean field theory for this task was initiated by Wolfram in [3]. Then, it was developed by Gutowitz [4], McIntosh [5], and Martínez [6] among many others. The idea is to model the long-term behaviour of density with a polynomial specified by the evolution rule of an ECA.

These polynomials are commonly nonlinear and are directly related to the dynamics of ECAs.

Another way to represent the dynamics of ECAs is using basins of attraction [7]. In this case, we have a graphic representation of all evolution in an ECA, and the branches and basins in these graphs describe the dynamics of the system. However, this technique can produce several basins for the same automaton and it is limited up to 32 cells because of the exponential growth.

On the other hand, recent papers have exposed numerical techniques for detecting chaotic behaviour in ECAs. These studies take a sample of evolutions to estimate Lyapunov exponents [8, 9, 10], response curves [11] and Fourier spectra [12]. In particular, ECAs have been analysed in [13] using a Walsh transformation in order to know their efficiency in the generation

* Corresponding author. Tel.: +52 7711426813.

E-mail addresses: jseck@uaeh.edu.mx (J.C. Seck-Tuoh-Mora), jmedina@uaeh.edu.mx (J. Medina-Marin), genaro.martinez@uwe.ac.uk (G.J. Martínez), nhromero@uaeh.edu.mx (N. Hernández-Romero).

of random sequences. A relationship between conserved quantities (density classification and nonequilibrium phase transition) and the dynamics of ECAs is presented in [14]; and empirical measures for the intermediate conservation degree of properties in ECAs have been proposed in [15].

With these results as background, the aim of this paper is to obtain a representation for the dynamical behaviour of density in ECAs by surface interpolation. We take the density and the binary value of configurations and their evolutions in an ECA, and with them we calculate two surfaces describing the dynamic behaviour of these values using the nearest-neighbour interpolation.

For a small number of cells (22 cells), all the configurations are taken. Thus, the surfaces obtained represent in a complete way the dynamics of density in time. Further, for a greater number of cells (100, 200 and 400), the surfaces are estimated with a sample of random configurations. In all these cases, we have analysed ECAs with periodic boundary conditions.

This process represents the dynamical behaviour of density in ECAs with two surfaces. Besides, these surfaces are analysed to detect periods in time and classify periodic, chaotic and complex behaviour in ECAs; obtaining interesting results.

The paper is organised as follows. Section 2 presents the definition of ECAs and shows the problems of analysing their dynamics with mean field theory and basins of attraction. Section 3 describes the process to obtain surfaces that describe the dynamical behaviour of density. It shows as well how these surfaces are studied to understand and classify the dynamics of ECAs. Section 4 explains how these surfaces are estimated for a greater number of cells taking a sample of evolutions; proposing a surface and histogram based classification of ECAs. Section 5 applies this classification to the 88 ECA representative rules. The final sections provide the discussion and the conclusions of the paper.

2. Preliminars

2.1. Elementary cellular automata

This paper is concerned with the analysis of elementary cellular automata with periodic boundary conditions in the terminology presented by [16,17].

An elementary cellular automaton (ECA) is defined by a finite array of locally connected cells x_i where $i \in \{0, \dots, n-1\}$ (ring of the integers modulo n) and each x takes a value from a binary set of states $\Sigma = \{0, 1\}$. A sequence of cells $\{x_i\}$ of finite length n is a configuration c of the ECA. The set of finite configurations is represented as Σ^n . An evolution is described by a sequence of configurations $\{c_i\}$ given by the mapping $\Phi : \Sigma^n \rightarrow \Sigma^n$ such that:

$$\Phi(c^t) \rightarrow c^{t+1} \quad (1)$$

where t indicates time and the sequence of cell states in c defines the global state. The cell states in c^t are updated simultaneously by the same evolution rule φ in the following way:

$$\varphi(x_{i-1}^t, x_i^t, x_{i+1}^t) \rightarrow x_i^{t+1} \quad (2)$$

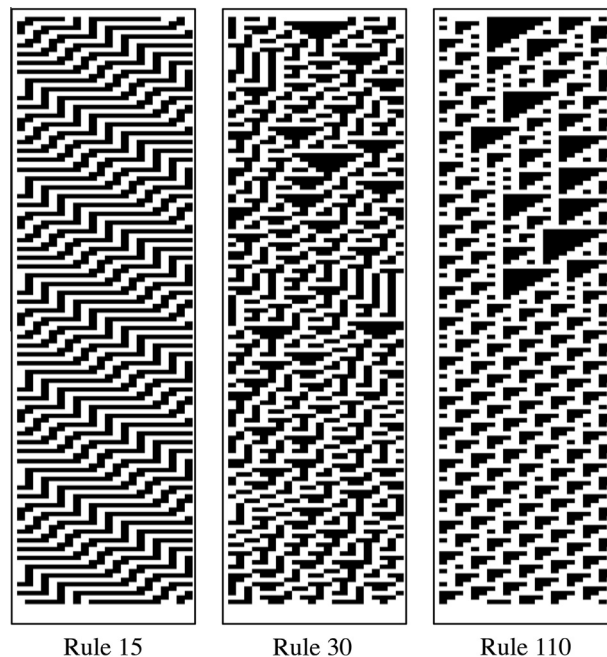
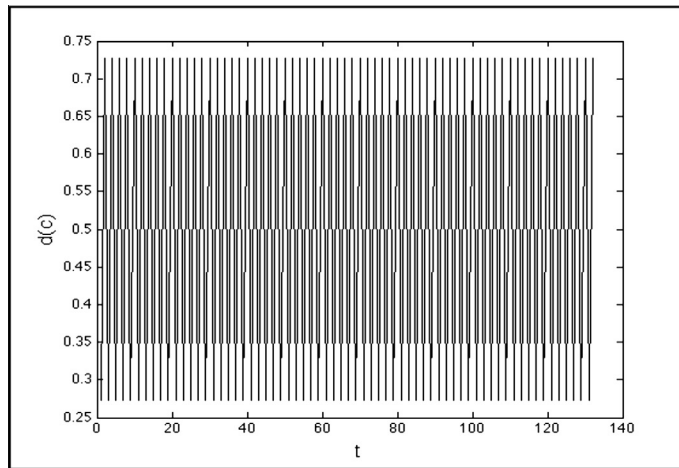
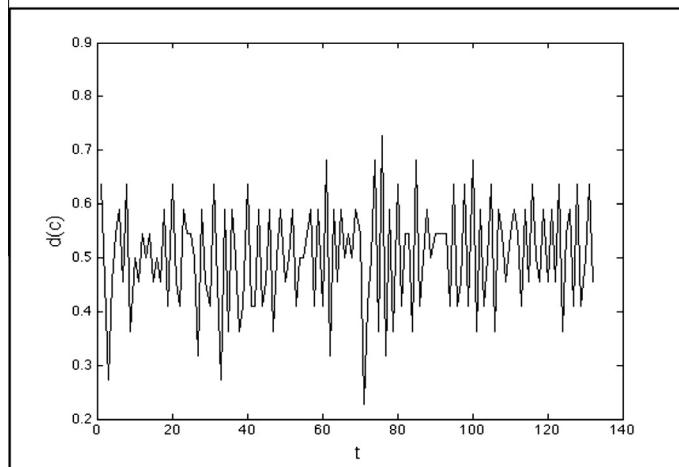


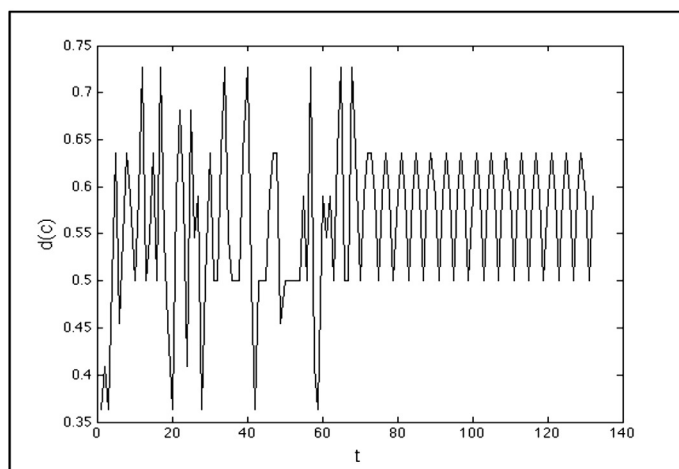
Fig. 1. Examples of evolutions in ECAs. In these evolutions we can see examples of periodic (rule 15), chaotic (rule 30) and complex dynamics (rule 110).



Rule 15



Rule 30



Rule 110

Fig. 2. Normalised density against time in the evolution of ECAs. Rule 15 has a periodic behaviour, rule 30 shows an aperiodic density dynamics and rule 110 presents a periodic behaviour after a number of steps.

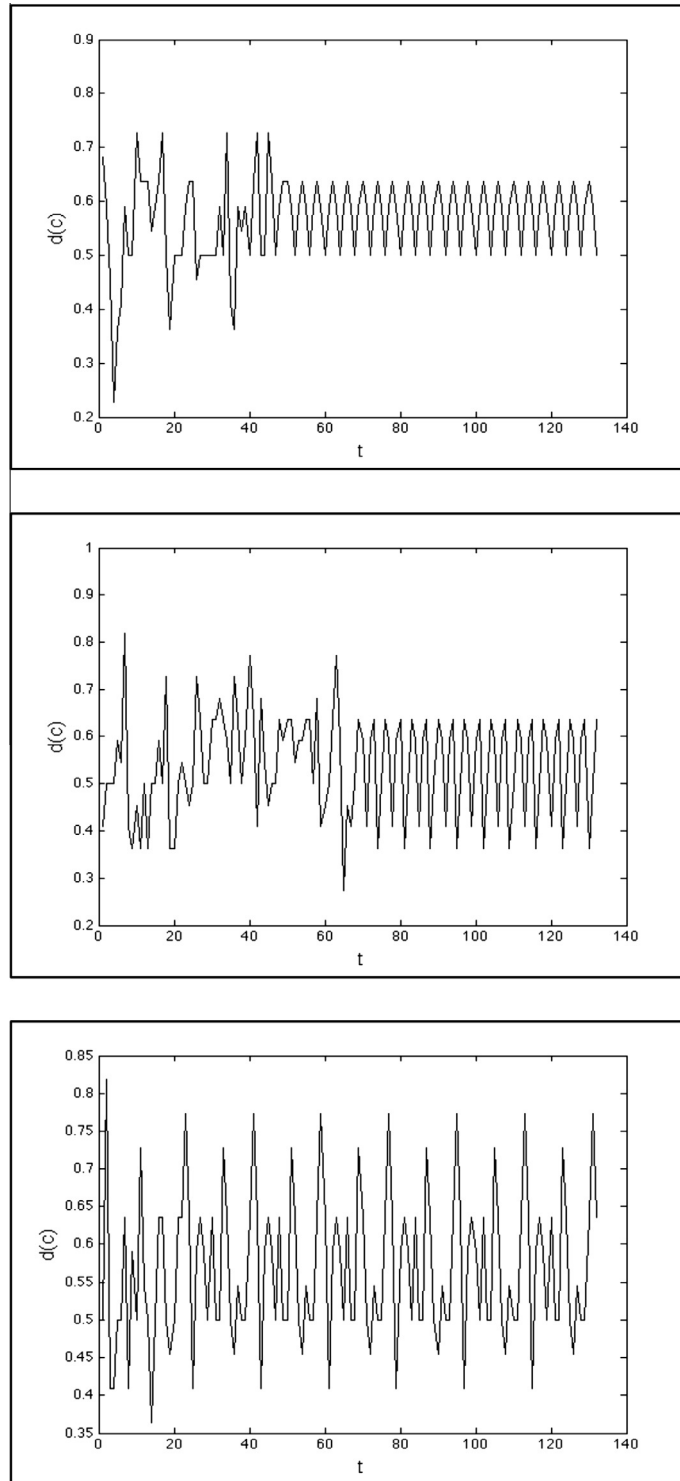


Fig. 3. Sequences of different periods in rule 110. These sequences exhibit the diversity of periodic structures produced by this ECA.

with the condition

$$x_i^t = x_j^t, \quad i \equiv j \pmod n$$

Thus in ECAs there are $2^3 = 8$ different neighbourhoods and $2^{2^3} = 256$ rules that are enumerated following Wolfram's notation [2].

2.2. Normalised density in ECAs

For every $c \in \mathbb{Z}^n$ let $\alpha(c)$ be the number of cells in state 1 and let $\beta(c)$ be the decimal value of the binary sequence represented by c . These values are normalised as follows:

$$d(c) = \alpha(c)/n \tag{3}$$

$$b(c) = \beta(c)/(2^n - 1) \tag{4}$$

The function $d(c)$ is the normalised density of c . This value is useful to describe the dynamical behaviour of an ECA even for a small number of cells because every evolution $\{c_i\}$ is also described by a sequence $\{d(c_i)\}$ of normalised densities. Fig. 1 shows the evolution of rules 15, 30 and 110 from random initial configurations of 22 cells and 132 time steps (dark cells in state 0 and light cells in state 1). We are taking $6n$ evolutions to obtain a better approximation for the long term behaviour of these ECAs. In computer experiments, we are using space–time diagrams with time going down.

Fig. 2 illustrates the associated sequences $\{d(c_i)\}$ against time. Each sequence $\{d(c_i)\}$ describes in an adequate way the dynamics of the original evolution. A *period* in $\{d(c_i)\}$ is the size of the final interval in which the sequence repeats its values. In these examples, rule 15, which is an ECA Class II in Wolfram’s classification, has a density sequence $\{d(c_i)\}$ of period 2. In the other cases, rule 30 (Class III) has an aperiodic density sequence; and rule 110 (Class IV) shows a final interval with period greater than 1.

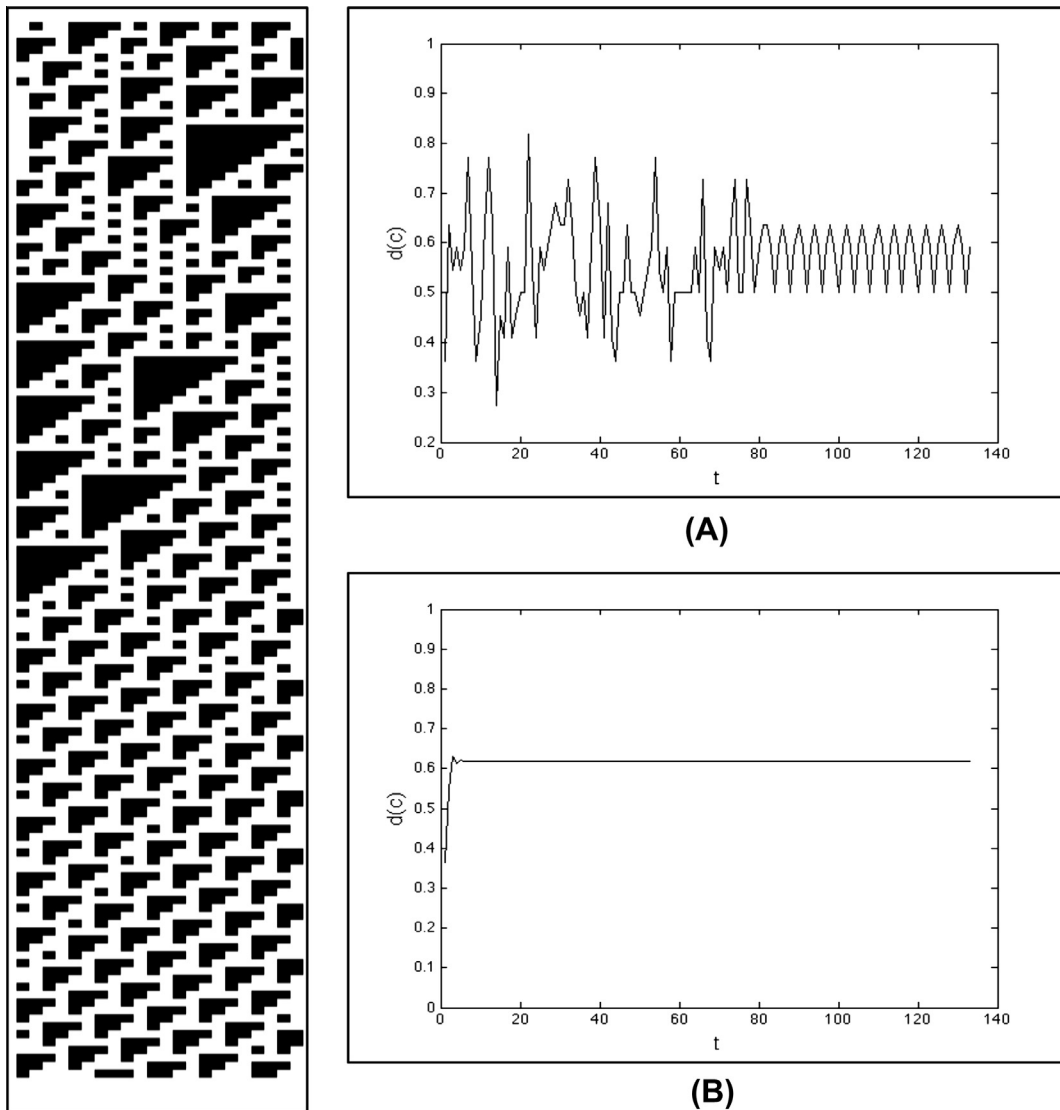


Fig. 4. Real density (A) and the mean field estimation (B) for the evolution of a random configuration in rule 110. We can see that the mean field estimation does not reflect the complex dynamics of this ECA.

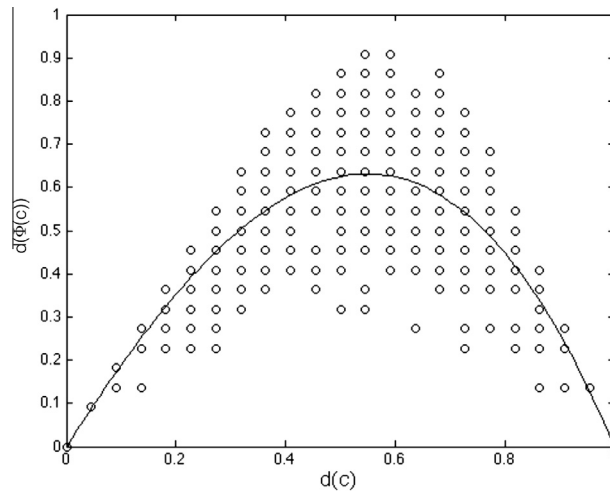


Fig. 5. Normalised density response (dots) in configurations of 22 cells and the estimation (continuous line) of the mean field polynomial in rule 110.

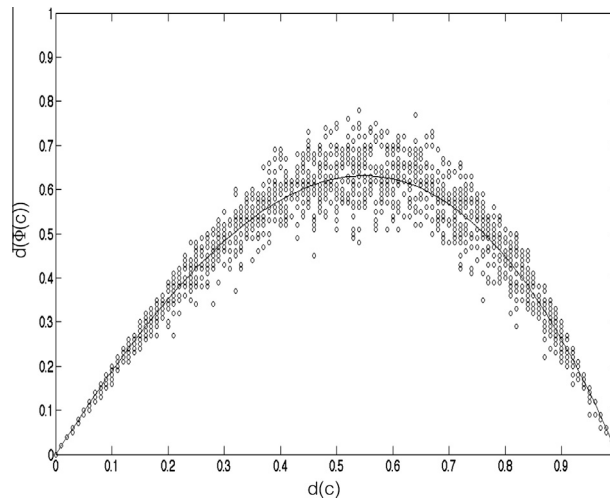


Fig. 6. Normalised density response (dots) in configurations of 100 cells and the estimation (continuous line) of the mean field polynomial in rule 110.

In fact, rule 110 presents density sequences of different periods (Fig. 3) due to 22 cells are enough to produce several types of non-trivial patterns as mobile self-localizations (or gliders) such as: $A, B, \bar{B}, C_1, C_2, C_3, D_1, D_2, E$ and \bar{E} [18]. Therefore, we can get a satisfactory approximation for the dynamical behaviour of ECAs if we have a good model for their densities.

2.3. Mean field approximation

Mean field theory has been used in ECAs to obtain general statistical properties without analysing evolution spaces of individual rules [19]. The method assumes that elements of Σ are independent and uncorrelated between each other in every neighbourhood. The probability of each neighbourhood is the product of the probabilities of its cells, and this probability defines part of the probability of the state in which the neighbourhood evolves in the following time step. Thus the probability of a state is estimated with the following polynomial.

$$p_{t+1} = P(p_t) = \sum_{i=0}^7 \varphi(X_i) p_t^v (q_t)^{3-v} \tag{5}$$

where i indexes every neighbourhood; X_i is a neighbourhood in Σ^3 , v indicates how often state 1 occurs in X_i , $3 - v$ shows how often state 0 occurs in X_i , p_t is the probability of a cell being in state 1 at time t , and $q_t = (1 - p_t)$ is the probability of a cell being in state 0.

To illustrate the polynomial with a particular example, in rule 255 we have that $\varphi(X_i) = 1$ for every i . If $p_t = 1$ then $q_t = 0$, so Eq. 5 has the next form:

$$\begin{aligned}
 P(p_t) &= 1q_t^3 + 1p_tq_t^2 + 1p_tq_t^2 + 1q_t p_t^2 + 1p_tq_t^2 + 1p_t^2q_t + 1p_t^2q_t + 1p_t^3 = q_t^3 + 3p_tq_t^2 + 3p_t^2q_t + p_t^3 \\
 &= 0^3 + 3(1 \cdot 0^2) + 3(1^2 \cdot 0) + 1^3 = 1
 \end{aligned}$$

Thus, the polynomial predicts that a configuration with $p_t = 1$ evolves into a new configuration with $p_{t+1} = 1$ in rule 255. In this example we can see that the polynomial depends on the neighbourhoods and the evolution rule, but not in the size of the configuration.

Let us take now rule 110 which has the following evolution rule:

$$\varphi_{R110} = \begin{cases} 1 & \text{if } 001, 010, 011, 101, 110 \\ 0 & \text{if } 000, 100, 111 \end{cases} \tag{6}$$

Therefore, the associated mean field polynomial is calculated as follows.

$$P(p_t) = 0q_t^3 + 1p_tq_t^2 + 1p_tq_t^2 + 1q_t p_t^2 + 0p_tq_t^2 + 1p_t^2q_t + 1p_t^2q_t + 0p_t^3 = 2p_tq_t^2 + 3p_t^2q_t \tag{7}$$

2.4. Mean field polynomial and temporal dynamics of density

The mean field polynomial is usually used to estimate the long term value of density in an ECA. For an initial configuration c_1 , the normalised density $d(c_1)$ represents the probability p_1 of a cell being in state 1. Thus, the dynamical behaviour of density can be estimated with the iteration of the mean field polynomial such that $d(c_{i+1}) = P(d(c_i))$. However, in some cases, it does not provide satisfactory results.

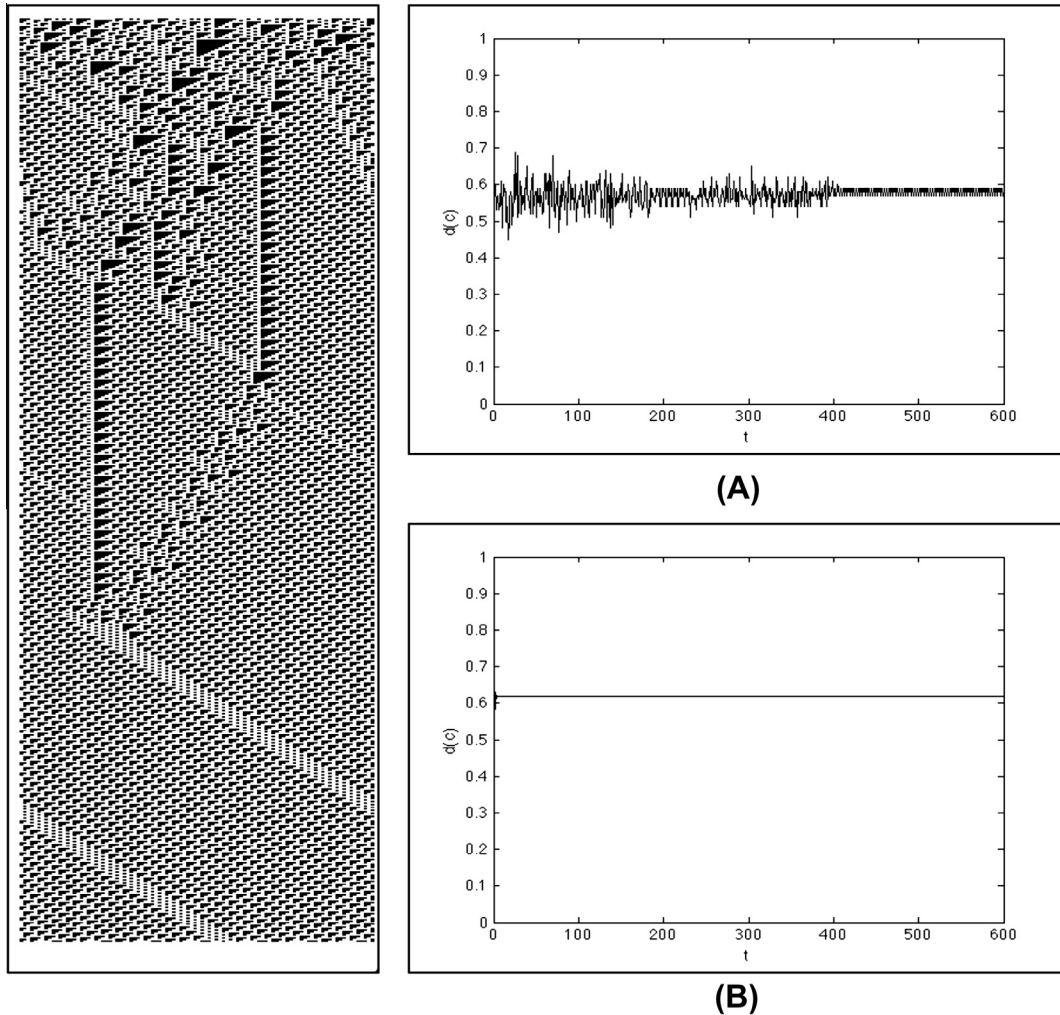


Fig. 7. Real density (A) and the mean field estimation (B) for the evolution of a random configuration of 100 cells with density 0.53 in rule 110. Even though the polynomial gives a good estimation for the density value, it does not reflect its periodic behaviour.

For instance, Fig. 4 shows the evolution in 132 steps of rule 110 for 22 initial cells with density $8/22$. It also presents the dynamics in time of the real normalised density and the step-by-step estimation with the polynomial in Eq. 7.

In this case, the iteration of the polynomial does not show the complexity in the dynamical behaviour of density. The main problem is that configurations with the same density are able to evolve in configurations with different densities; that is, density is not a function in most ECAs.

This is illustrated in rule 110 taking a sample of different configurations in Σ^{22} with the same density; and varying the density from 0 up to 1 with step 0.01. Fig. 5 displays the experimental values of $d(c)$ against $d(\Phi(c))$ (dots) and compares them with the estimation of the mean field polynomial for every density (continuous line).

If we take a sample of configurations with a bigger number of cells (100), the mean field approximation has a better estimation (Fig. 6).

Nevertheless, the dynamics predicted by the polynomial does not capture the periodic behaviour, even in a qualitative way, of the normalised density produced by an initial configuration of 100 cells in 600 steps (Fig. 7).

2.5. Analysing the dynamics of ECAs

The best way to describe the dynamics of finite ECAs is with the basins of attraction defined by Wuensche [7]. These are a complete representation for the evolution of an ECA, and their properties describe the dynamical features of the automaton. However, they are restricted to a few tens of cells for their computational requirements, and an ECA may have several basins of attraction to analyse.

There are as well other papers devoted to the numerical detection and study of chaotic and complex behaviours in ECAs. For instance, to calculate Lyapunov exponents, response curves and Fourier spectra [8] [11] [9] [10] [12]. In these works, a sample of evolutions is taken to obtain an estimation of these parameters.

Based on the previous works, this paper proposes the application of surface interpolation to model the temporal dynamics of density in ECAs.

For a small number of cells, we measure the normalised density and binary values of each configuration and their evolutions. The binary value is useful to order sequences with the same density.

With them, we generate two surfaces by interpolation, one modelling the response of density, and the other one describing the response of the binary value. For a larger number of cells (hundreds), a sample of the configurations is taken to estimate both surfaces.

With the process described above, we are able to characterise the dynamic behaviour of the density in ECAs with a compact description; using only two surfaces.

3. Surface interpolation

The previous section shows that density response is not a function. To solve this problem, we take the normalised binary value $b(c)$ for each sequence to obtain a function. For a small number of cells n , the following algorithm produces surfaces describing the dynamics of density and binary values in ECAs.

Algorithm 1.

1. For every $c \in \Sigma^n$, compute a table where the first two columns keep the values $d(c)$ and $b(c)$, and the last two columns keep the values $d(\Phi(c))$ and $b(\Phi(c))$.

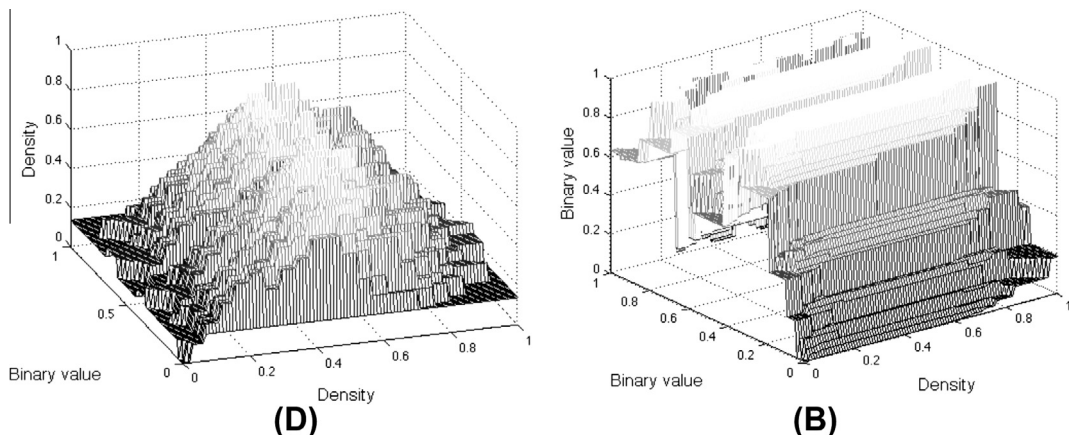


Fig. 8. Surfaces describing the response for normalised density (D) and binary value (B) in rule 110.

2. Generate the surface D to estimate the normalised densities using the nearest-neighbour interpolation, where the independent values are the first two columns of the table and the values for the interpolation are the ones in the third column.
3. Generate the surface B to estimate the normalised binary values using the nearest-neighbour interpolation, where the independent values are the first two columns of the table and the values for the interpolation are the ones in the fourth column.

We are using the nearest-neighbour interpolation because it is a very simple method which approximates an unknown point into the nearest known point on a surface. This kind of interpolation is an extension of Voronoi diagrams to adjust surfaces with a sample of points [20].

The nearest-neighbour interpolation will provide always a correct answer for the estimated densities and binary values because it is taking all the possible configurations to produce the surface.

We use Matlab® R2012b to perform our experimental results. In particular, the interpolation surfaces are obtained with the command `TriScatteredInterp()`. Fig. 8 shows the surfaces obtained with configurations of 22 cells for rule 110.

With these surfaces we can estimate the sequences $\{d(c_i)\}$ and $\{b(c_i)\}$ such that:

$$\begin{aligned} d(c_{i+1}) &= D(d(c_i), b(c_i)) \\ b(c_{i+1}) &= B(d(c_i), b(c_i)) \end{aligned} \tag{8}$$

In this way, we can obtain the dynamic behaviour of density with the iteration of these surfaces. Fig. 9 presents the real and estimated densities for a random configuration of 22 cells and 132 steps in rule 110.

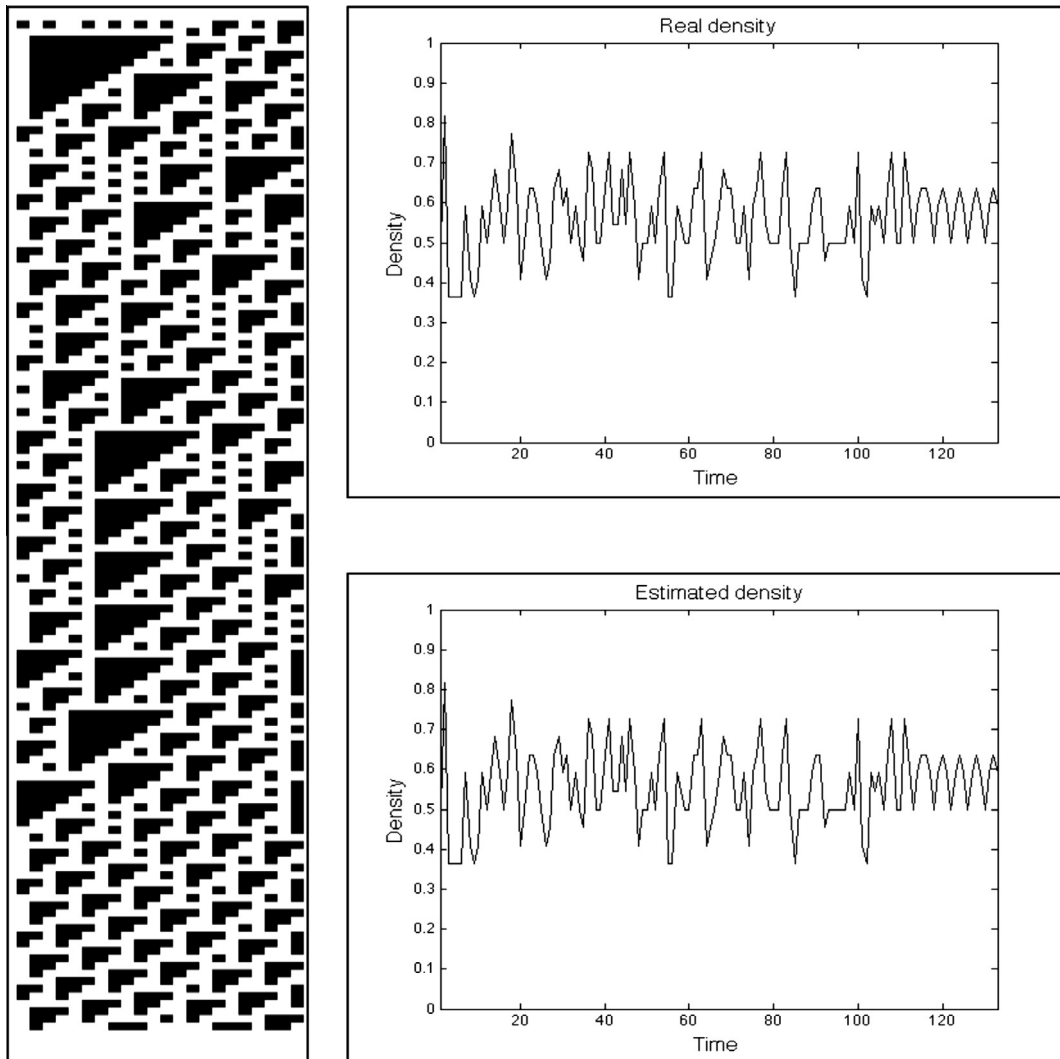


Fig. 9. Real and estimated densities for a random configuration. We have an exact prediction of the density behaviour using the surfaces D and B .

Both graphs are identical in Fig. 9, showing that the surfaces are estimating the exact value of density in time. This is consequence that the surfaces are calculated using all the configurations in Σ^{22} ; therefore, every possibility is considered. Fig. 10 presents the density surfaces obtained for 22 cells for rule 15 (reversible and Class II), rules 22, 30 and 90 (Class III) and rules 54 and 110 (Class IV).

It is clear in Fig. 10 that the smoothness of a surface is related to the complexity of the dynamic behaviour in each ECA.

3.1. Long term range and difference surfaces

The surfaces D and B can be analysed to characterise the dynamics of an ECA. For instance, for $0.01 \leq i, j \leq 0.99$ with a step of 0.01, we can take pairs (i, j) of normalised densities and binary values, and iterate them in the surfaces. Densities

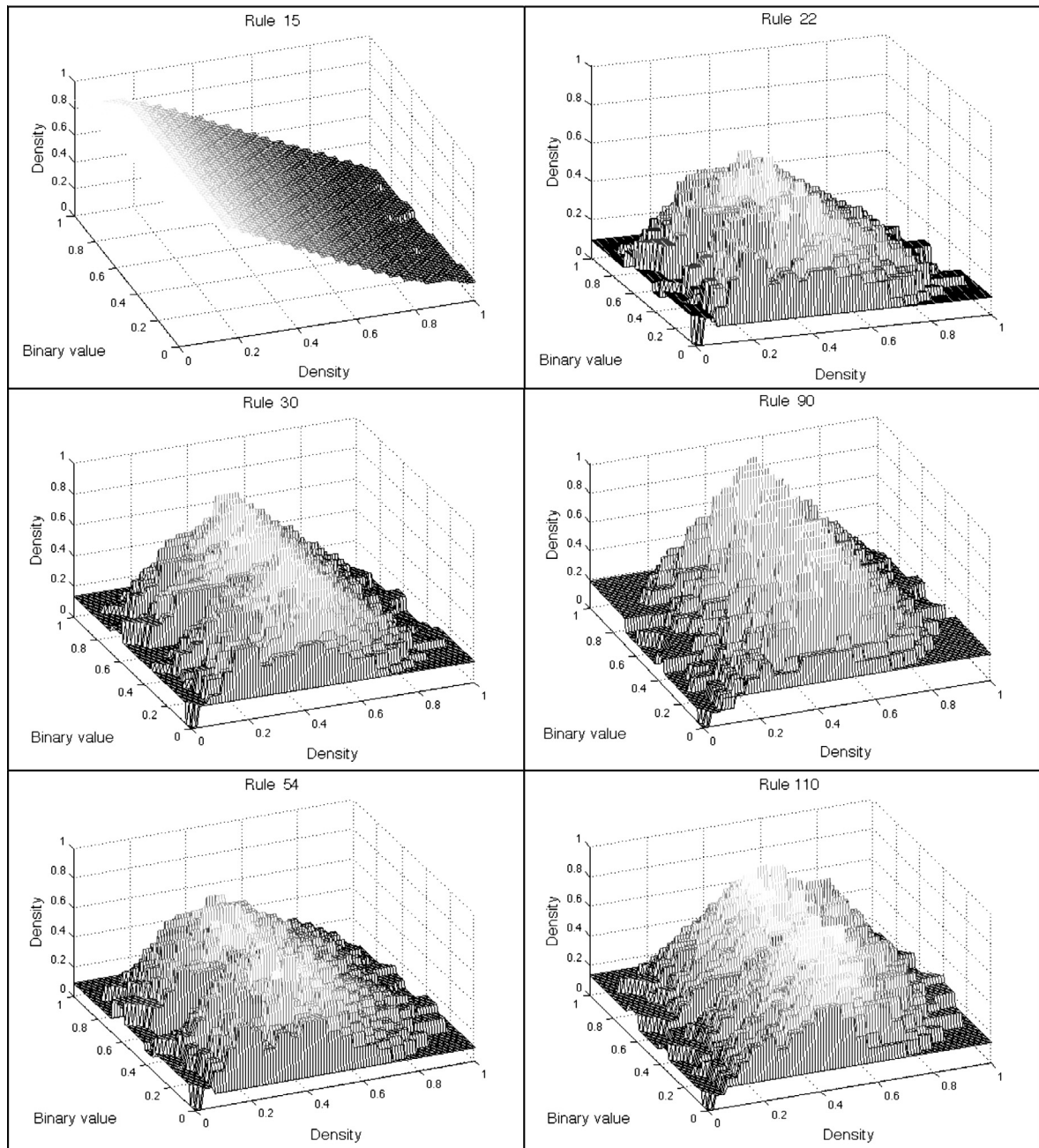


Fig. 10. Density surfaces for different ECAs. For periodic ECAs we have almost-plain surfaces, and for chaotic and complex ECAs we obtain steep and rugged surfaces.

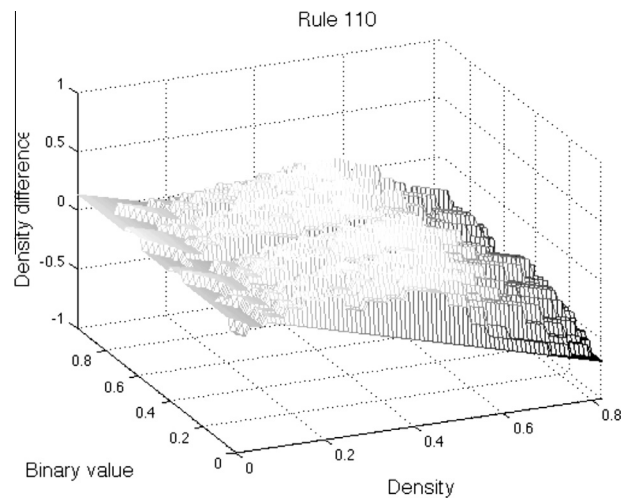


Fig. 11. Surface of the density difference for rule 110. In the surface we can notice that configurations with high density have a relevant decrement of 1's in the next generation. However, configurations with low and mean densities have a small increment of 1's.

0 and 1 are not taken in the initial pairs because they only evolve into fixed configurations; and we are looking for configurations with more interesting behaviour.

Then we take the minimum and maximum values of every parameter to estimate their long term range. With the surface D , we can take the difference of density in one step for every pair (i, j) in these ranges. This process yields a new surface E such that:

$$E(i, j) = D(i, j) - i \quad (9)$$

The surface E represents the density difference in one step for the values inside the long term range. For rule 110, 132 iterations of every pair (i, j) produce a density range $[0, 0.82]$ and a binary value range $[0, 0.98]$. The corresponding surface E is depicted in Fig. 11.

Fig. 11 shows that density decreases notably in the evolution of configurations with high density; however, for configurations with low and mean densities, we have a small increment of density in their evolutions. Fig. 12 presents the difference surfaces for 22 cells for rule 15 (reversible and Class II), rules 22, 30 and 90 (Class III) and rules 54 and 110 (Class IV).

Fig. 12 shows that periodic ECAs produce planar surfaces; that is, the changes in density are not complex. It is interesting that chaotic rules (30 and 90) have more complicated difference surfaces than complex rules (54 and 110). On the other hand, rule 22 has a difference surface similar to rule 54. Perhaps rule 22 needs more cells to show a chaotic behaviour.

3.2. Histogram of periods

With the surfaces D and B we can take a sample of m initial values (i, j) and iterate them q times in the surfaces to obtain a sequence of estimated densities and detect periods in the last p iterations of density to approximate and analyse its long term behaviour. Exact repetitions of the values of $d(c)$ are considered for the estimation of periods.

The m periods can be classified in a histogram. If the histogram has only a few types of short periods, the ECA is not producing a complex dynamics. A majority (but not only) of short periods could indicate that the ECA is producing structures of different periods, which is related to mobile self-localizations and complex behaviours. If the histogram shows a majority of long periods or aperiodic evolutions, then the ECA is producing chaotic evolutions.

Taking again the rule 110 and their surfaces D and B for $n = 22$ cells, we iterate 400 initial values (i, j) for $6n = 132$ steps; and we detect periods for the last $2n = 44$ iterations. The associated histogram is showed in Fig. 13.

Fig. 13 shows several periods and aperiodic sequences detected in rule 110, and most of them are short periods; as expected for this kind of ECA. Fig. 14 presents the histograms of periods obtained for 22 cells for rule 15, rules 22, 30 and 90; and rules 54 and 110.

Fig. 14 illustrates that periodic ECAs produce sequences with very short periods. Chaotic rules (30 and 90) have histograms where long periods and aperiodic evolutions are dominant. Complex rules (54 and 110) have a majority of short periods. Finally, the histogram of rule 22 shows only short periods despite of being chaotic; this indicates that this ECA needs more cells to expose a chaotic behaviour.

4. Surface estimation for a greater number of cells

Similar to the case of basins of attraction [21], a complete representation using surfaces is not possible for more than 32 cells. However, we can take a sample of configurations and their evolutions to estimate the corresponding surfaces.

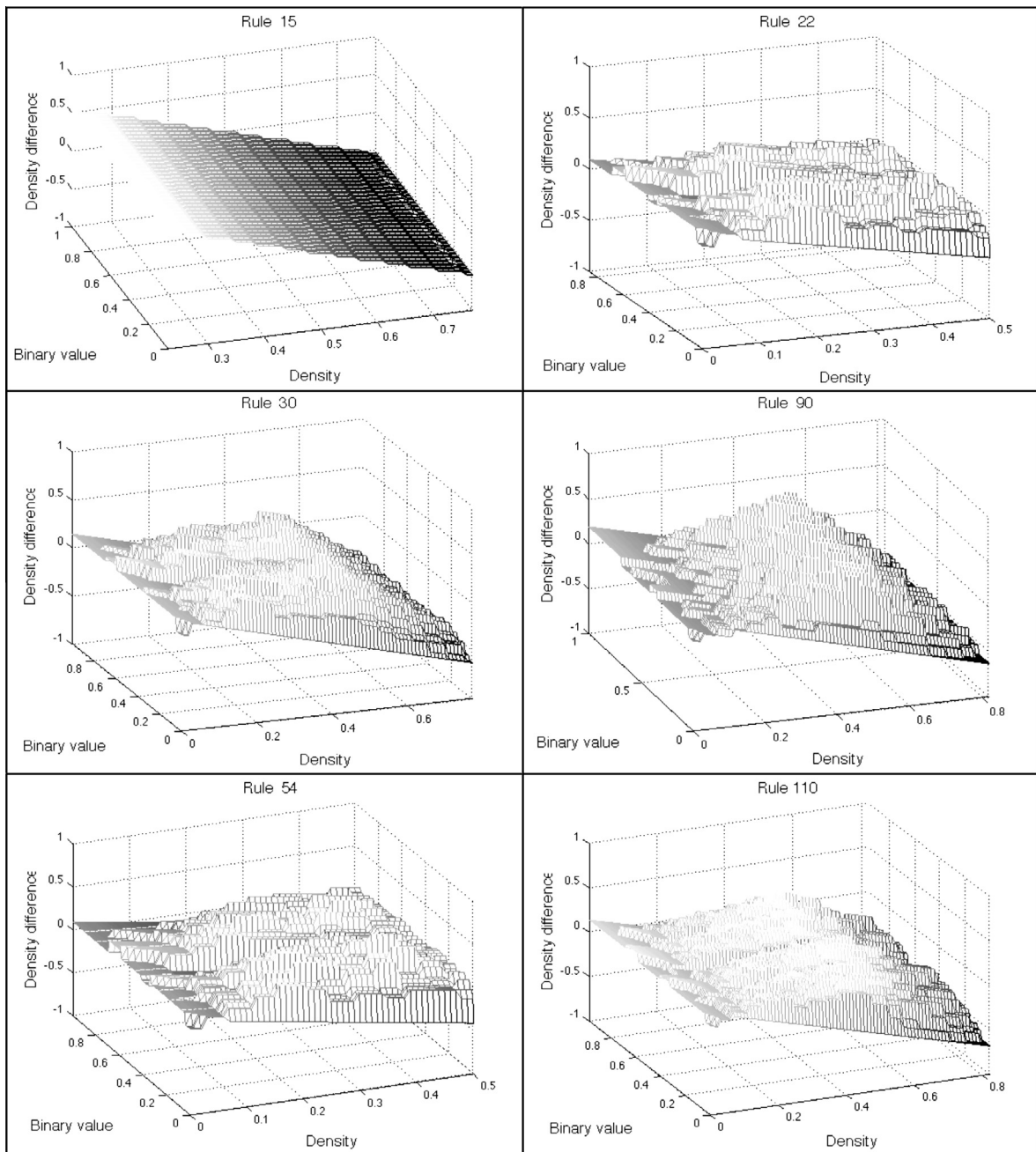


Fig. 12. Difference surfaces for different ECAs. Class II ECAs show planar surfaces, meanwhile chaotic and complex ECAs present more complicated surfaces.

The objective of this estimation is to obtain a qualitative approximation for the dynamics of density in ECAs for larger configurations (with hundreds of cells), rather than obtaining an exact model of this behaviour.

In fact, it is very difficult to obtain a precise model because of the difference between the exponential growth in the number of configurations and the feasible size (in terms of memory and processing time) of a sample for calculating the surfaces.

However, the idea is that the surfaces reflect the essence of the density dynamics in ECAs.

With the expansion of the surfaces for a greater number of cells, we are looking for a method to classify the density dynamics in a qualitative way. That is, the behaviour predicted by the surfaces would be characterised for very short periods for ECAs producing fixed and periodic evolutions. Long periods or aperiodic behaviour would be the main attribute of ECAs with chaotic behaviours. Finally, we would have a mixture of short and long periods for ECAs producing different periodic structures in a steady background.

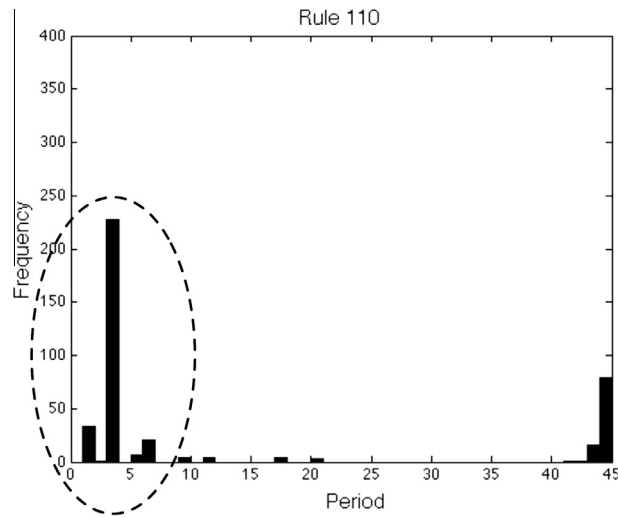


Fig. 13. Histogram of periods for rule 110. This ECA has a majority (but not only) of short periods.

The algorithm for n cells is defined as follows.

Algorithm 2.

1. For every $i \in I = \{1/n, 2/n, 3/n, \dots, (n-1)/n\}$, take m random initial configurations with density i .
2. For every initial configuration c , take its evolution $\Phi^{2n}(c)$.
3. Add configurations with density 0 and 1. Thus we have a total of $2m(n-1) + 2$ configurations.
4. Remove identical configurations keeping one of them in the configuration set. This set represents a sample of initial and long term configurations.
5. For every configuration c in this set, calculate its evolution $\Phi^{n/2}(c)$.
6. Make a table with four columns, the first two columns keep the normalised densities and binary values of the configurations and the last two columns keep the same values for their evolutions after $n/2$ steps.
7. Generate the surface D to estimate the normalised density using the nearest-neighbour interpolation where the independent values are the first two columns of the table and the values for the interpolation are the ones in the third column.
8. Generate the surface B to estimate the normalised binary values using the nearest-neighbour interpolation where the independent values are the first two columns of the table and the values for the interpolation are the ones in the fourth column.

In the modelling of nonlinear systems, it is used to distinguish between the transient and the stable dynamical states. This kind of analysis has been applied to cellular automata as well [7,22–24].

In areas devoted to model and control nonlinear dynamical systems [25,26], sometimes the proposed model takes into account both the transient and the steady dynamics to estimate in a better way the behaviour of the system.

Previous papers studying dynamical properties in cellular automata [9–12,14,27–30] have used a different number of cells and evolutions (from tens to thousands). In most of them, for n cells, these studies have used a number of evolutions close to n .

Empirically, one can suppose that for n cells, in n evolutions we can observe the effect of all the initial cells over every cell in the n -th evolution.

In order to obtain surfaces that present a more accurate qualitative description for the density dynamics in ECAs, we will select a sample combining random configurations and configurations obtained after $2n$ evolutions. In this way, the surfaces will model the transient and the steady behaviour of ECAs with a sample that can be calculated in a reasonable time.

With this sample of configurations, we are taking their evolutions in $n/2$ steps in Algorithm 2 in order to estimate the surfaces. Once more, we do this for obtaining a better estimation for the transient and the steady dynamics of the density in ECAs.

Again, we make use of the function `TriScatteredInterp()` in Matlab® R2012b to calculate the surfaces D and B with the previous algorithm.

In Algorithm 2 we have m configurations and their evolutions in $2n$ steps for each density ($2m$ configurations in total). Since there are $n-1$ different densities (distinct to 0 and 1) we have $2m(n-1)$ configurations for the estimation of the surfaces. Adding the extreme cases of configurations with density 0 and 1, we are taking a total of $2m(n+1) + 2$ configurations to approximate D and B . For bigger values of n and m , we obtain surfaces with a better approximation, but requiring more

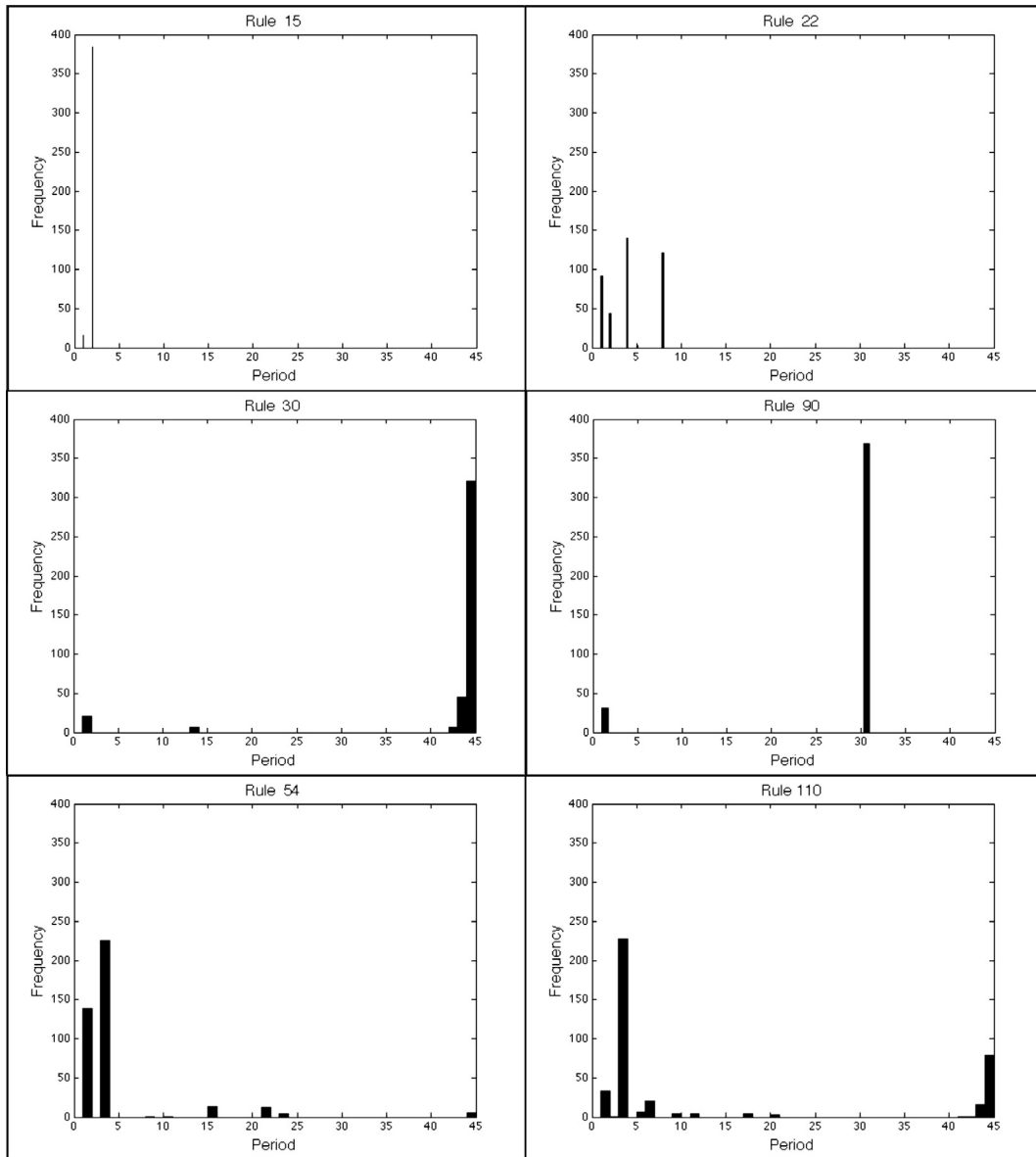


Fig. 14. Histogram of periods for different ECAs. Rule 15 shows only very short periods. Complex ECAs (rules 54 and 110) present a diversity of periods, most of them of short length. Chaotic ECAs (rule 30 and 90) have a majority of long periods. One exception is rule 22 which displays a majority of short periods although it is a chaotic ECA. Perhaps it needs more than 22 cells to show its real behaviour.

time to be calculated. For $m = 600$ and $n = 100$, Algorithm 2 takes around four minutes in order to calculate the surfaces. For $n = 200$ it takes around 18 min; and for $n = 400$ it takes around two hours.

With these surfaces, we compute the histogram of periods with the following algorithm.

Algorithm 3.

1. Take k pairs (i, j) of initial densities and binary values.
2. For each pair, keep a sequence of $2n$ iterations in the surfaces to estimate the behaviour of density in $2n$ steps.
3. Take the last n values of each sequence to detect a period from 1 to $n - 1$. If the sequence is aperiodic then it will have period n .
4. Form a histogram with the k periods.

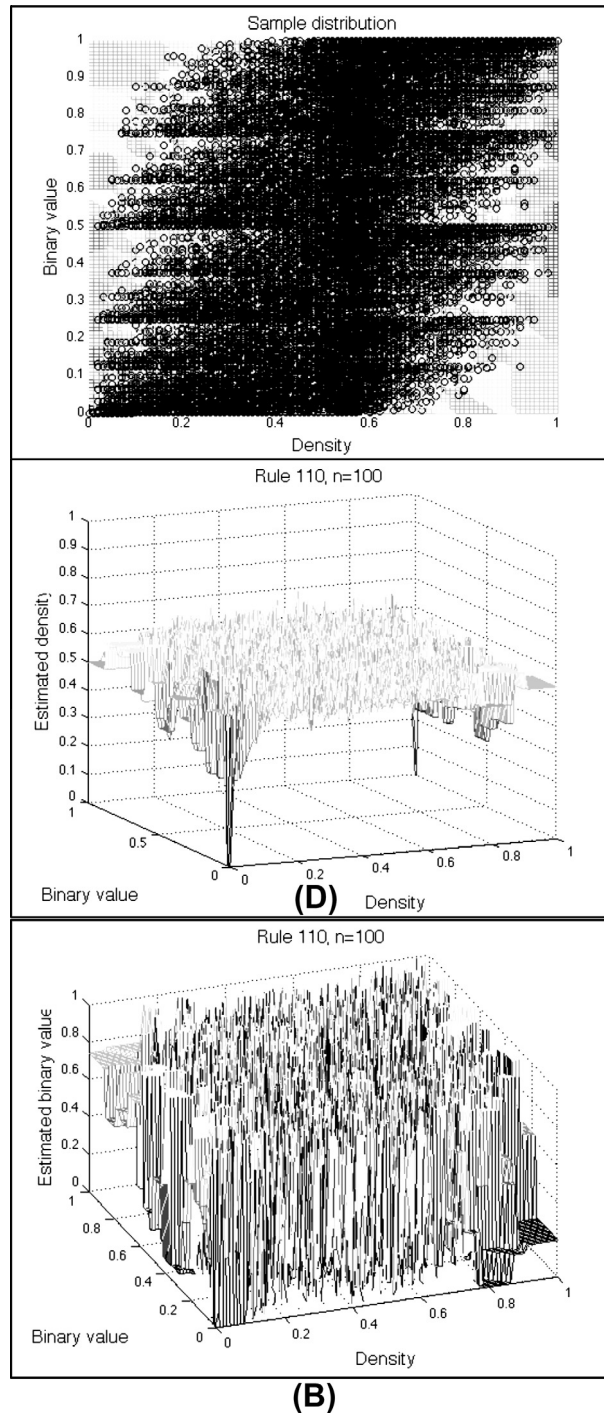


Fig. 15. Estimated surfaces D and B for 100 cells in rule 110. The surface D shows that the density tends to 0.6, but the roughness of D and B indicates that the evolutions of this ECA do not have a trivial behaviour.

In [Algorithm 3](#) we use surfaces D and B to approximate the dynamics of density after $2n$ iterations. We have to remember that every iteration in the surfaces is estimating the density obtained after $n/2$ evolutions. This means that the $2n$ iterations are approximating the density dynamics of $2n(n/2) = n^2$ evolutions (with intervals of size $n/2$) in order to calculate roughly its long term behaviour.

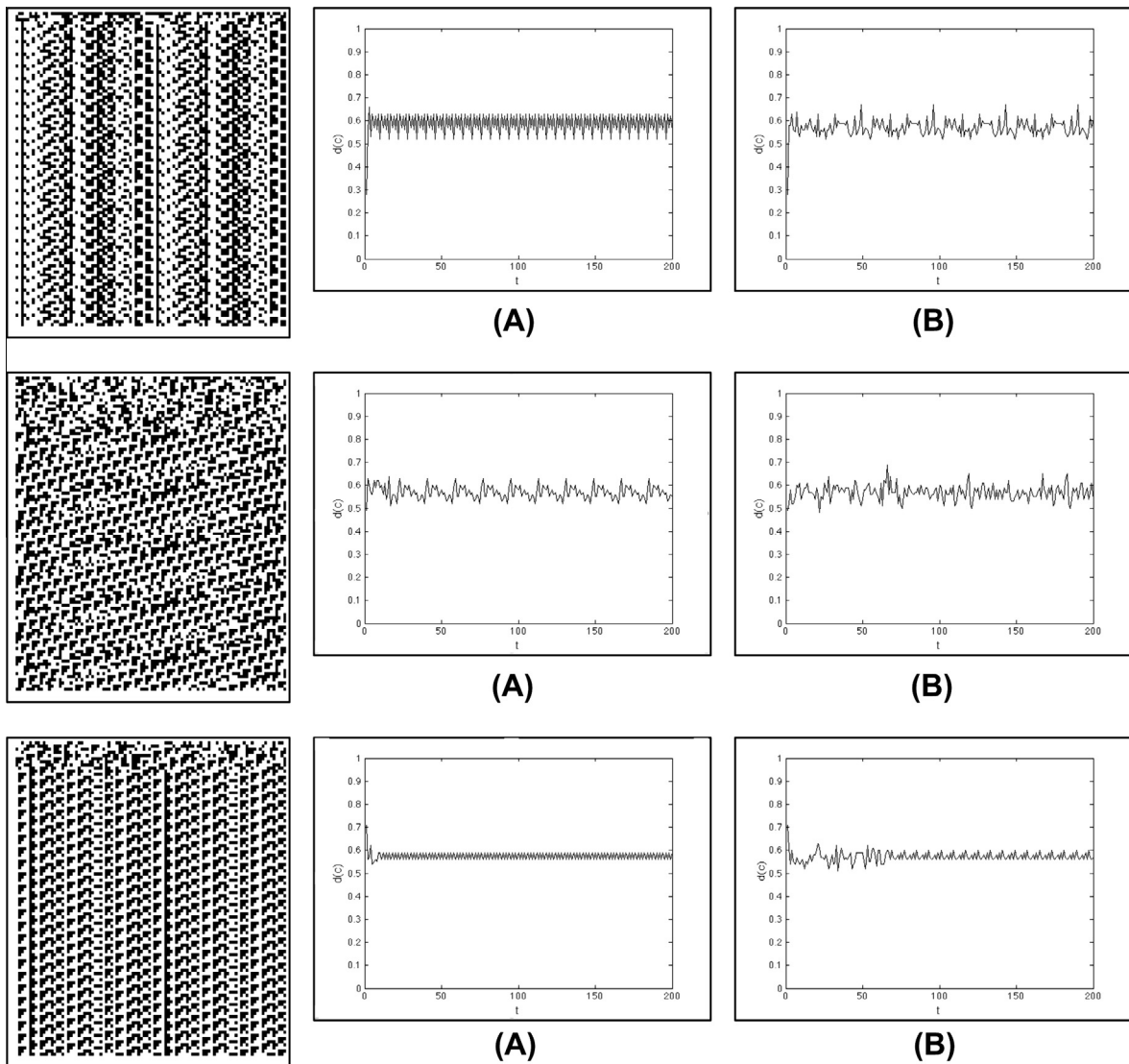


Fig. 16. Real (A) and estimated (B) density dynamics with surfaces D and B for three random initial configuration with $n = 100$ in rule 110. The evolutions, real and estimated temporal densities are taken every 50 steps following Algorithm 2. The space–time diagrams show only 100 configurations in steps of 50 evolutions for simplicity. We can see that the surfaces estimate different periods for distinct dynamical behaviours, achieving a good qualitative approximation.

In the previous algorithms, we calculate a sample of configurations trying to take into account the most possible regions of normalised densities and binary values. Let us take again the rule 110; for $n = 100$ and $m = 600$, one execution of Algorithm 2 produces the surfaces in Fig. 15. The figure displays as well the distribution of the pairs to interpolate the surfaces.

In this case, we initially calculate $2m(n - 1) + 2 = 118802$ configurations; after deleting repetitions, we finally got 107712 configurations for the interpolation. These surfaces are rougher than those in Fig. 8 because they are estimations. We approximate the surface of 2^{100} different configurations with only 107712 points; that is, with only the 8.4970×10^{-24} percent of possible values.

Fig. 16 shows the estimations obtained by the surfaces calculated with Algorithm 2. They approximate, in a qualitative way, the dynamics of density for three different evolutions with $n = 100$ in rule 110. As we said before, every iteration on the surfaces estimates 50 evolutions of the ECA. In this way, 200 iterations in the surfaces estimate 10000 evolutions. The space–time diagrams display *compressed* evolutions (only 100 configurations for simplicity) where there are 50 steps between one configuration and the following one. The experimental densities are taken in the same way, every 50 steps.

In this example we can see that the surfaces do not give an exact approximation for the real periods, but they estimate different periods for the different kinds of real density dynamics. So the complex behaviour of this ECA can be classified in a qualitative way.

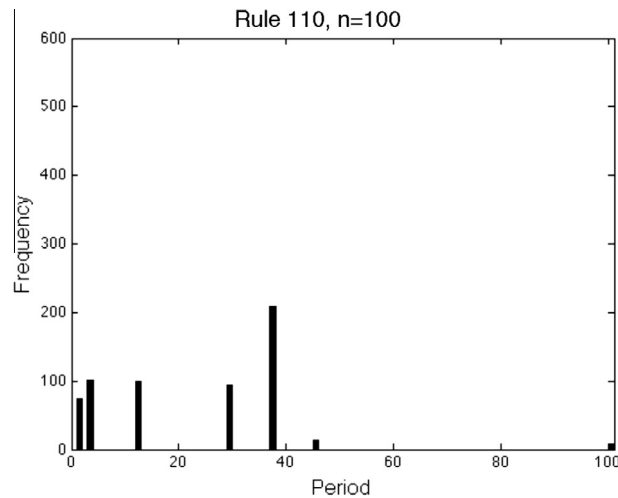


Fig. 17. Histogram of estimated periods for rule 110. The estimated frequencies suggest that the ECA produces several structures with different density periods.

Since we are only taking a minimum part of all the possible configurations, an initial pair (i, j) of density and binary values will tend to reach a period after some iterations. With the histograms, we can classify ECAs in the following types:

- (A) Most of the sequences have very short periods; their frequencies are close to the left margin of the histograms. The associated ECAs produce simple structures with almost no variation of density.
- (B) Most of the sequences generate long periods or are aperiodic; their frequencies are in the right side of the histograms. The corresponding ECAs have chaotic evolutions with high variations of density.
- (C) Most of the sequences produce a variety of short and medium-length periods; most of their frequencies are distributed in the left side of the histograms. The ECAs in this class have evolutions characterised by several structures where density varies in different periods.

These types of ECAs can be related to Wolfram's classification in a qualitative way. Class I and II are associated with ECAs type A, Class III with type B; and Class IV (or particularly, ECAs producing gliders) with type C.

Fig. 17 exposes the histogram for rule 110 with $n = 100$ and $k = 600$.

The histogram shows several short and medium-length periods as expected for a complex ECA. For $n = 100, 200$ and 400 ; and $k = 600$, Fig. 18 presents the estimated density surfaces for rules 15, 22, 30, 90, 54 and 10.

For these ECAs, the histograms of estimated periods are presented in Fig. 19. These histograms illustrate the expected behaviour for every class of ECA. The periodic ECA (rule 15) shows a majority of periods 1 and 2; chaotic ECAs (rule 22, 30 and 90) have a majority of aperiodic iterations or periods in the right side of the histogram. Finally, complex ECAs (rule 54 and 110) expose a majority of periods in the left side of the histogram; most of them are periods greater than 1 or 2.

The surfaces and histograms obtained with the previous algorithms are based on a minimum sample of configurations; therefore, the results so obtained are just approximations for the real behaviour of ECAs and we lost precision as we take a greater number of cells.

5. Atlas of surfaces and histograms in ECAs

Figs. 20–22 display the estimated surfaces with $n = 100$ for the 88 representative ECAs. Fig. 23 presents the histograms associated only to ECAs type B or C. The rest of ECAs have *trivial* histograms showing one or two very short periods, as the case of rule 15. Therefore, they are not included in the figure.

The surfaces and the histograms offer some interesting results:

1. ECAs normally categorised as Class I (rules 0, 8, 32, 40, 128, 136, 160 and 168) have estimated surfaces largely defined by horizontal planes.
2. Reversible ECAs (rules 15, 51, 170 and 204) have estimated surfaces defined by 45-degree inclined planes. Rules 29 and 184 also have this kind of estimated surfaces. This means that these rules are density conservative for an even number of evolutions.

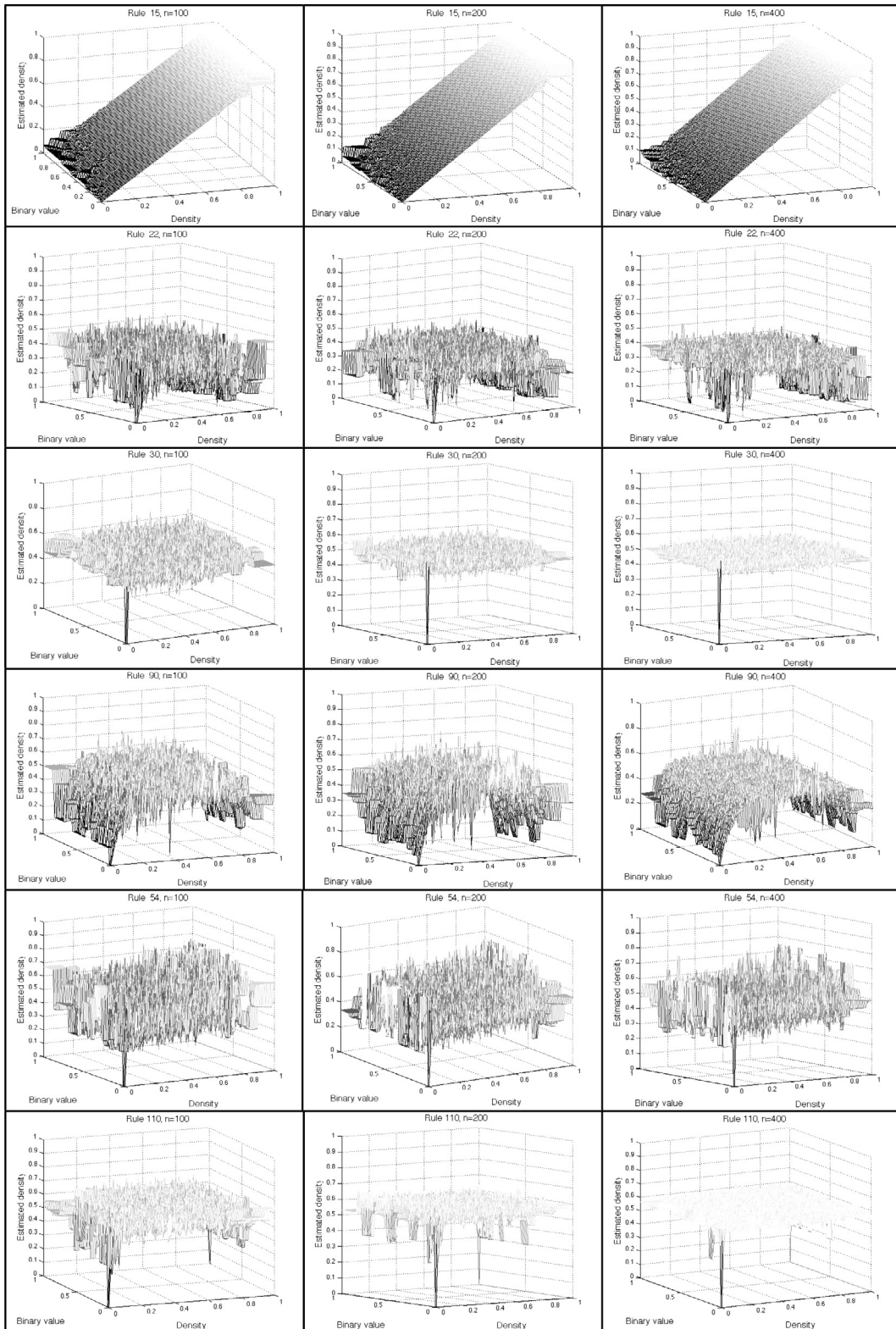


Fig. 18. Estimated density surfaces for different ECAs. Rule 15 (periodic ECA) has a plain surface. Chaotic and complex ECAs show very intricate surfaces, with exception of rule 30 and 110 for $n = 400$. Thus, we need to review the histograms of periods in order to classify the dynamics of density.

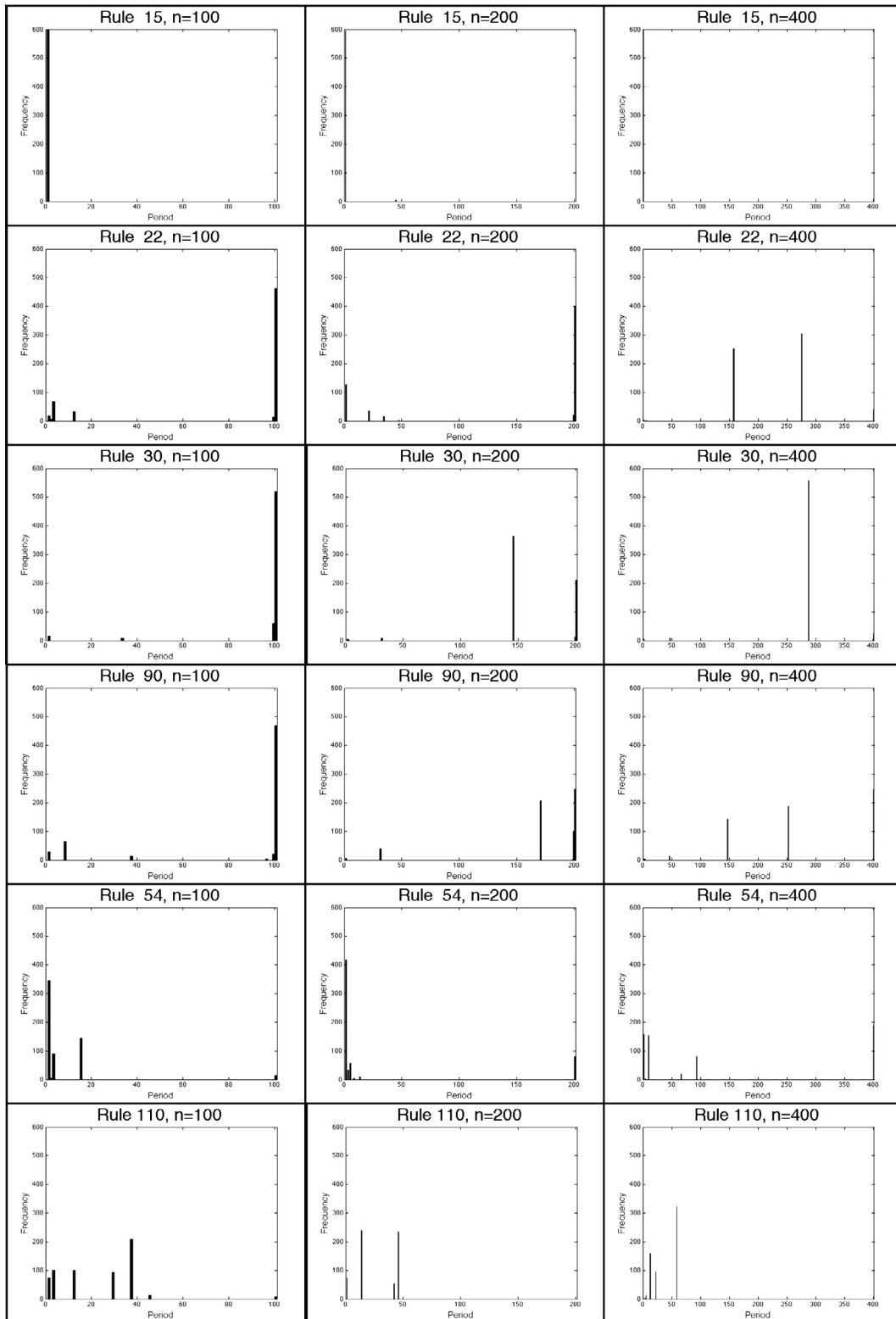


Fig. 19. Histograms of estimated periods for different ECAs. Rule 15 shows only unitary periods, rules 22, 30 and 90 have a majority of periods close to the right side of the histograms, which implies evolutions with chaotic structures. Rules 54 and 110 present a majority of periods in the left side of the histogram, suggesting the existence of different structures with distinct density periods in their evolutions.

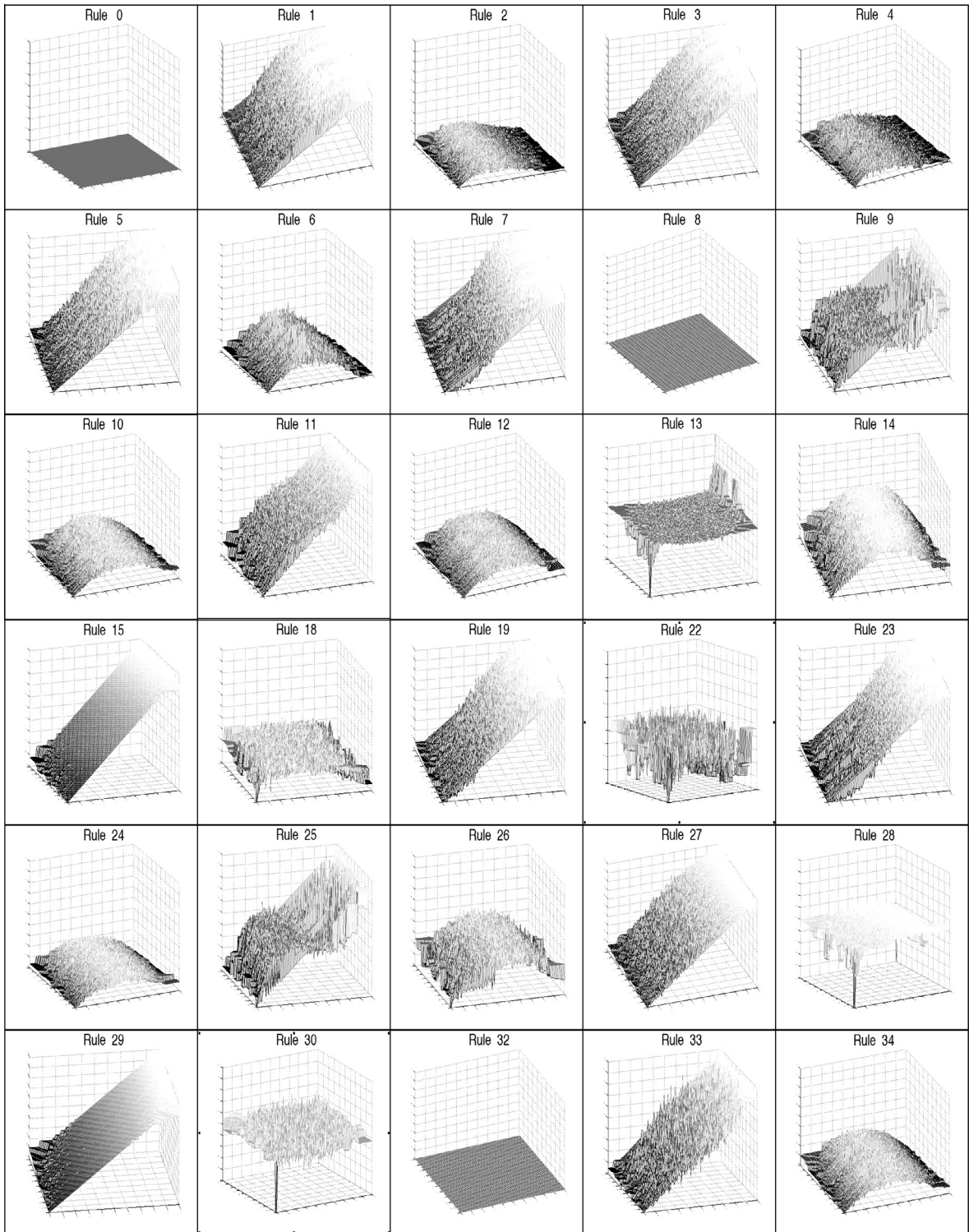


Fig. 20. Estimated surfaces for rules 0 to 34.

3. Two Class II rules (26 and 154) are classified as type B. These ECAs form isolated periodic structure whose period depend on the distribution of states in the initial configuration. Fig. 24 depicts some examples of evolutions in these ECAs and the behaviour of density in time.

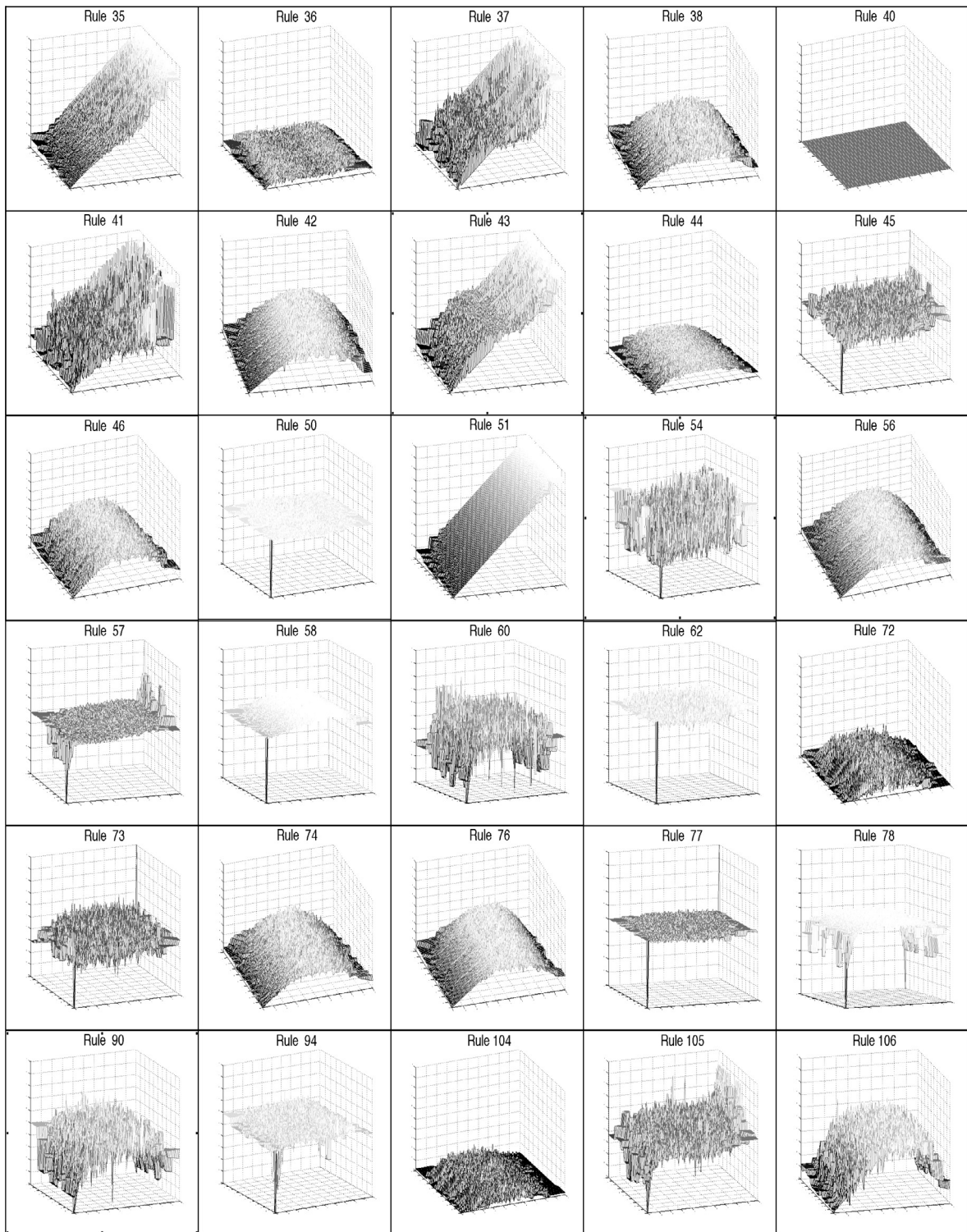


Fig. 21. Estimated surfaces for rules 35 to 106.

4. Two Class II rules (62 and 73) are classified as type C. The first ECA produces simple self-mobile structures in a periodic background. The second ECA generates isolated vertical structures of different periods. Examples of evolutions and density behaviour is presented in Fig. 25.

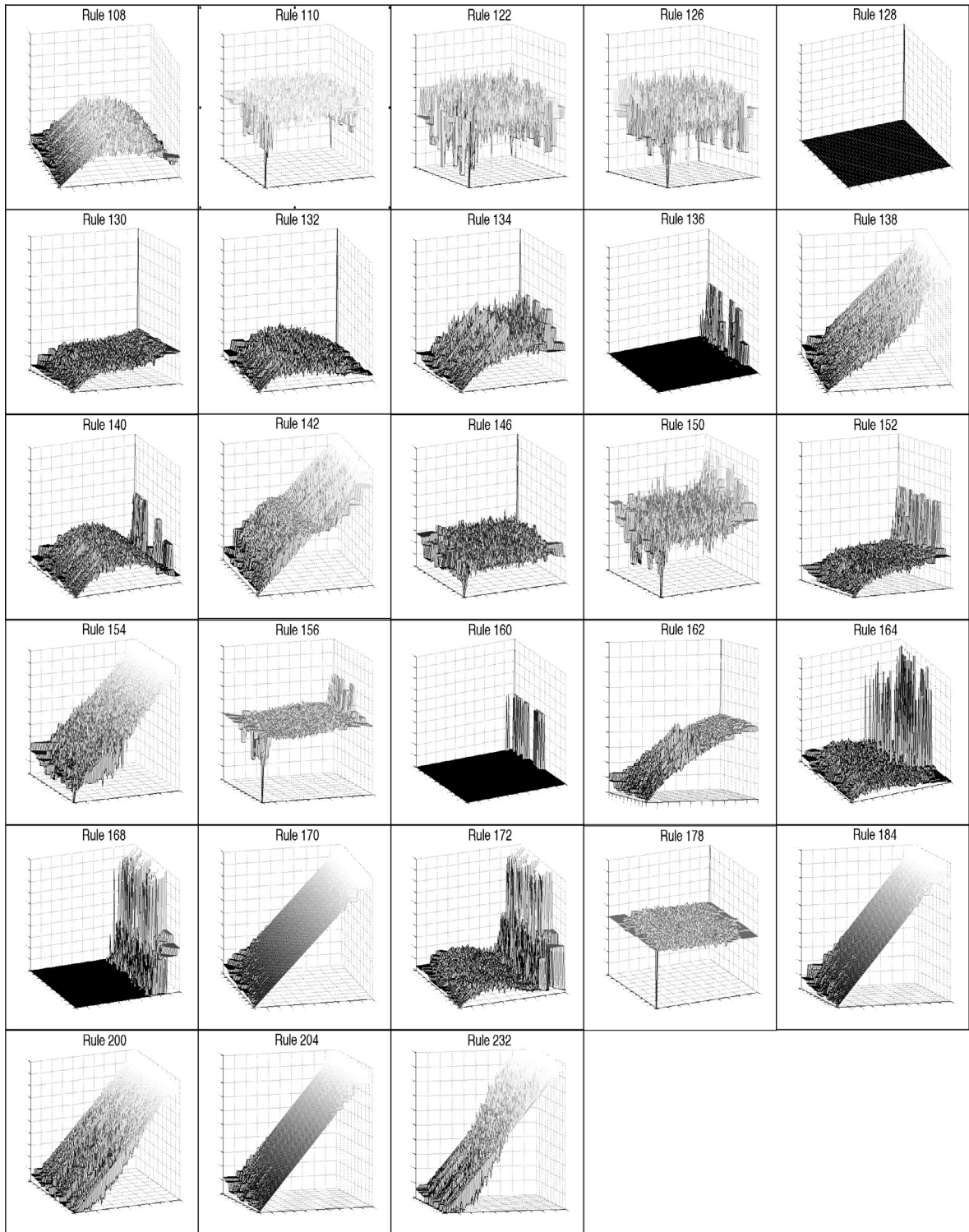


Fig. 22. Estimated surfaces for rules 108 to 232.

Table 1 shows the classification of the 88 representative ECAs with regard of their estimated density dynamics. The different types of ECAs are compared with Wolfram's classification.

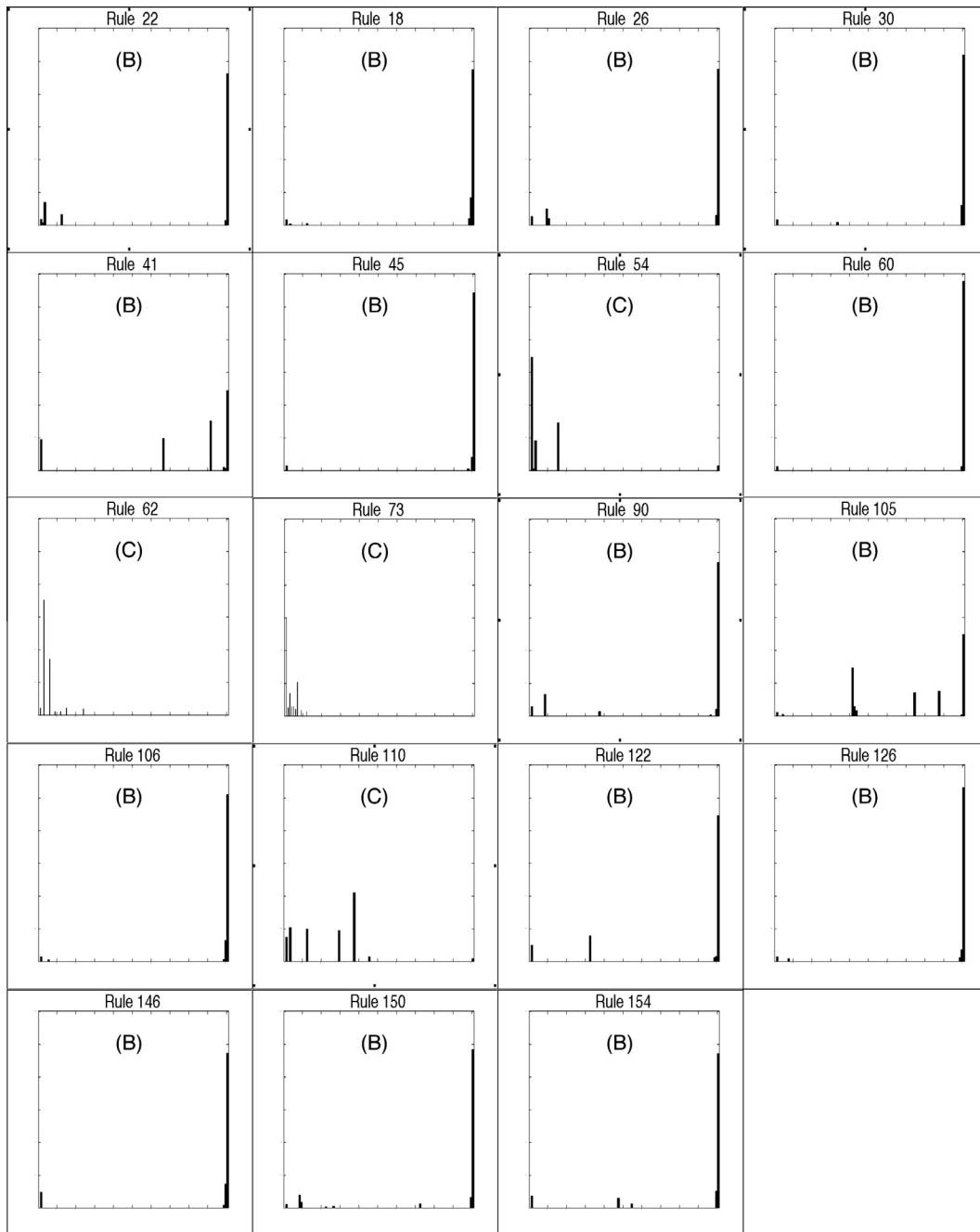


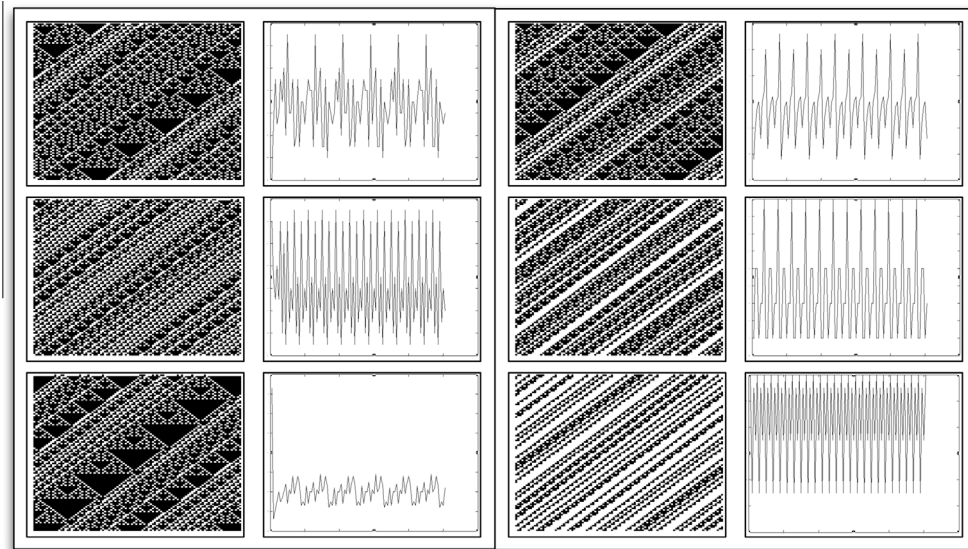
Fig. 23. Histograms of estimated periods for ECAs type B and C. These ECAs show a nontrivial behaviour in their density dynamics.

6. Discussion

This work has considered the value of a binary sequence to obtain a function for the density in ECAs. This function is modelled by surface interpolation, thus we obtain two surfaces, one for density and the other for binary values.

For a small number of cells, the surfaces can be calculated so that they capture the entire behaviour of an ECA. With this, we are able to reproduce the exact dynamics of density in time. Besides, we obtain a compact representation (only two surfaces) to model the density behaviour of ECAs.

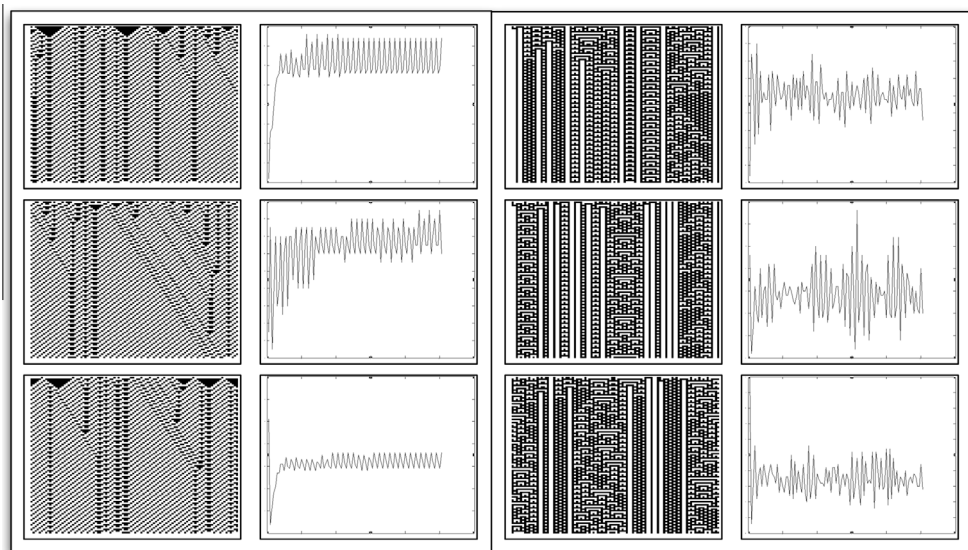
These surfaces are useful to estimate the long term ranges of density and binary values, and calculate the difference surface to analyse the behaviour of density in ECAs.



Rule 26

Rule 154

Fig. 24. Evolutions and density behaviour in rules 26 and 154.



Rule 62

Rule 73

Fig. 25. Evolutions and density behaviour in rules 62 and 73.

The most relevant analysis described in this paper is the histogram of periods. The process of taking a sample of initial pairs of density and binary values, and iterate them in the surfaces; is very useful to estimate the periods produced by ECAs. The histogram is able to classify the frequency and length of these periods, giving an approximation for the dynamic behaviour of ECAs.

This process can be extended for hundreds of cells to have a rough estimation about the dynamics of ECAs. In this way, periodic ECAs produce histograms with a majority of periods 1 and 2; in chaotic ECAs, the histograms show a majority of long periods or aperiodic sequences. Finally, complex ECAs generate histograms with a majority of short and medium periods.

Algorithm 3 takes only $2n$ iterations (instead of $6n$) and detect periods in the last n values (instead of $2n$) to save computational resources. Nevertheless, with these values we obtain satisfactory results in the analysis and classification of ECAs. Therefore, the present analysis offers a numerical tool to automatically classify and recognise ECAs displaying complex behaviour, chaos, or periodic behaviour.

Table 1

Classification of the 88 representative ECAs according to their estimated density dynamics (EDD) and the comparison with Wolfram's classification (W).

Rule	EDD	W									
0	A	I	26	B	II	56	A	II	132	A	II
1	A	II	27	A	II	57	A	II	134	A	II
2	A	II	28	A	II	58	A	II	136	A	I
3	A	II	29	A	II	60	B	III	138	A	II
4	A	II	30	B	III	62	C	II	140	A	II
5	A	II	32	A	I	72	A	II	142	A	II
6	A	II	33	A	II	73	C	II	146	B	III
7	A	II	34	A	II	74	A	II	150	B	III
8	A	I	35	A	II	76	A	II	152	A	II
9	A	II	36	A	II	77	A	II	154	B	II
10	A	II	37	A	II	78	A	II	156	A	II
11	A	II	38	A	II	90	B	III	160	A	I
12	A	II	40	A	I	94	A	II	162	A	II
13	A	II	41	B	IV	104	A	II	164	A	II
14	A	II	42	A	II	105	B	III	168	A	I
15	A	II	43	A	II	106	B	IV	170	A	II
18	B	III	44	A	II	108	A	II	172	A	II
19	A	II	45	B	II	110	C	IV	178	A	II
22	B	III	46	A	II	122	B	III	184	A	II
23	A	II	50	A	II	126	B	III	200	A	II
24	A	II	51	A	II	128	A	I	204	A	II
25	A	II	54	C	IV	130	A	II	232	A	II

7. Conclusions

The analysis of cellular automata is still open to the application of numerical tools commonly used in other fields in order to obtain new models and results in the dynamics of these systems. The approach presented in this paper shows that simple concepts developed in other areas offer interesting results when are applied in the study of cellular automata.

Further work implies the extension of the process described in this manuscript for a larger number of cells. Every configuration has a unique binary value, but it is difficult to calculate when hundreds of cells are taken. With the process previously presented, we need a way to order configurations with the same density and not the calculus of a complete binary value.

Other kinds of surface interpolations could be useful to obtain better estimations for the dynamic behaviour of ECAs; and defining ways to discriminate configurations with the same density in two or three dimensions would extended this process for cellular automata in higher dimensions.

The results presented in this manuscript have been focused on the analysis of density in ECAs. Nevertheless, a further study can be developed taking now the binary value $b(c)$. These results could be compared and complemented with the ones obtained by [31] in order to classify ECAs based on the temporal dynamics of binary values.

Finally, the methods presented in this paper could be modified to be applied in cellular automata with a bigger number of states or different from the classical specification. For instance, probabilistic cellular automata [32] or cellular automata with memory [33,34]. Besides, other kind of complex systems could be analysed with these methods, as coupled map lattices and random boolean networks [32,35]. In these cases, perhaps more than two surfaces should be calculated for modelling the densities of distinct states, or mapping continuous spaces to binary sequences in a similar way to [31] so that we can use the analysis exposed in this paper.

References

- [1] Tommaso T, Norman M. Cellular automata machines. Cambridge, Massachusetts: The MIT Press; 1987.
- [2] Wolfram S. A new kind of science. Wolfram Media; 2002.
- [3] Wolfram S. Statistical mechanics of cellular automata. Rev Mod Phys 1983;55:601–44.
- [4] Gutowitz H, Langton C. Mean field theory of the edge of chaos. In: Morán F, Moreno A, Merelo JJ, Chacón P, editors. Proceedings of the third european conference on advances in artificial life. Springer-Verlag; 1995. p. 52–64.
- [5] McIntosh HV. Wolfram's class IV and a good life. Phys D 1990;45:105–21.
- [6] Martínez GJ, Seck-Tuoh-Mora JC, Zenil H. Computation and universality: class IV versus class III cellular automata. J Cell Autom 2012;7:393–430.
- [7] Wuensche A, Lesser M. The global dynamics of cellular automata. Addison-Wesley Publishing Company; 1992.
- [8] Shereshevsky MA. Lyapunov exponents for one-dimensional cellular automata. J Nonlinear Sci 1992;2:1–8.
- [9] Baetens JM, De Baets B. A Lyapunov view on the stability of cellular automata. In: Zenil H, editor. Irreducibility and computational equivalence. Springer; 2013.
- [10] Baetens JM, De Loof K, De Baets B. Influence of the topology of a cellular automaton on its dynamical properties. Commun Nonlinear Sci 2013;18:651–68.
- [11] Fuks H, Skelton A. Response curves for cellular automata in one and two dimensions: an example of rigorous calculations. Int J Nat Comput Res 2010;1:85–99.
- [12] Ruivo ELP, de Oliveira PPB. A spectral portrait of the elementary cellular automata rule space. In: Zenil H, editor. Irreducibility and computational equivalence. Springer; 2013.

- [13] Martin B. A Walsh exploration of elementary CA rules. *J Cell Autom* 2008;3:145–55.
- [14] Takesue S. Characteristic dynamics of elementary cellular automata with a single conserved quantity. *J Cell Autom* 2008;3:123–44.
- [15] Schranko A, de Oliveira PPB. Towards the definition of conservation degree for one-dimensional cellular automata rules. *J Cell Autom* 2010;5:383–401.
- [16] Jen E. Cylindrical cellular automata. *Commun Math Phys* 1988;118:569–90.
- [17] Cinkir Z, Akin H, Siap I. Reversibility of 1D cellular automata with periodic boundary over finite fields \mathbb{Z}_p . *J Stat Phys* 2011;143:807–23.
- [18] Regular expressions for mobile self localizations in Rule 110 are presented in: <<http://uncomp.uwe.ac.uk/genaro/rule110/listPhasesR110.txt>>.
- [19] McIntosh HV. One dimensional cellular automata. UK: Luniver Press; 2009.
- [20] Aurenhammer F, Klein R. Voronoi diagrams. In: Sack JR, Urrutia J, editors. *Handbook of computational geometry*. North-Holland; 2000. p. 201–90.
- [21] Wuensche A. *Exploring discrete dynamics*. Luniver Press; 2011.
- [22] Gutowitz Transients HA, cycles, and complexity in cellular automata. *Phys Rev A* 1991;44:78817884.
- [23] Li W. Phenomenology of nonlocal cellular automata. *J Stat Phys* 1992;68:829–82.
- [24] Ilchinski A. *Cellular automata: a discrete universe*. World Scientific; 2001.
- [25] Ong C-M. *Dynamic simulation of electric machinery: using Matlab/Simulink*. Prentice-Hall; 1998.
- [26] Ogata K. *Modern control engineering*. Pearson; 2010.
- [27] Nakajima K, Haruna T. Self-organized perturbations enhance class IV behavior and 1/f power spectrum in elementary cellular automata. *BioSystems* 2011;105:216224.
- [28] Lizier JT, Prokopenko M, Zomaya AY. Coherent information structure in complex computation. *Theory Biosci* 2012;131:193203.
- [29] Baetens JM, Van der Weeen P, De Baets B. Effect of asynchronous updating on the stability of cellular automata. *Chaos Soliton Fract* 2012;45:383394.
- [30] Martínez GJ, Adamatzky A, Alonso-Sanz R. Complex dynamics of elementary cellular automata emerging from chaotic rules. *Int J Bifurcation Chaos* 2012;22.
- [31] Amigó JM, Zambrano S, Sanjuán MAF. Permutation complexity of spatiotemporal dynamics. *EPL Europhys Lett* 2010;90:10007.
- [32] Just W. Phase transitions in coupled map lattices and in associated probabilistic cellular automata. *Phys Rev E* 2006;74:046209.
- [33] Stone C, Bull L. Evolution of cellular automata with memory: the density classification task. *Biosystems* 2009;97:108–16.
- [34] Seck-Tuoh-Mora JC, Martínez GJ, Alonso-Sanz R, Hernández-Romero N. Invertible behavior in elementary cellular automata with memory. *Inf Sci* 2012;199:125–32.
- [35] Wittmann DM, Hock S, Theis FJ. Truth-content and phase transitions of random boolean networks with generic logics. *SIAM J Appl Dyn Syst* 2013;12:315–51.